UMDNJ-NEW JERSEY MEDICAL SCHOOL

2012 SUMMER STUDENT RESEARCH PROGRAM
REPORT OF ACCOMPLISHMENTS
SUMMER STUDENT ABSTRACTS

ROBERT L. JOHNSON, MD, FAAP
THE SHARON AND JOSEPH L. MUSCARELLE ENDOWED DEAN

WILLIAM C. GAUSE, PH.D.
SENIOR ASSOCIATE DEAN FOR RESEARCH

DEBORAH A. LAZZARINO, PH.D.
ASSISTANT DEAN FOR RESEARCH ADMINISTRATION

MS. GIOVANNA COMER
PROGRAM COORDINATOR

2012 SUMMER STUDENT RESEARCH PROGRAM

REPORT OF ACCOMPLISHMENTS/SUMMER STUDENT ABSTRACTS

ACKNOWLEDGEMENT

WE LIKE TO EXPRESS OUR

GRATITUDE AND APPRECIATION

TO THE NEW JERSEY MEDICAL SCHOOL ALUMNI

AND

THE FOUNDATION OF UMDNJ

FOR THEIR GENEROUS FINANCIAL SUPPORT!!

THE SUCCESS OF THIS PROGRAM DEPENDS

UPON YOUR CONTINUED FINANCIAL CONTRIBUTIONS.

2012

STUDENT ABSTRACTS

REPORT OF ACCOMPLISHMENTS

Table of Contents

PREFACE

For many years the New Jersey Medical School First-Second Year Students and Volunteers have participated in this organized research program. This program gives an opportunity for students and volunteers to work alongside an NJMS Faculty Mentor on a specific research project for a period of eight weeks. Over the eight week period the participants are exposed to the dynamic nature of biomedical science. During this time they learn about the methodology and results of laboratory/clinical research; sharpen diagnostic skills, and learn the value and limits of experimental results. This program has been fortunate to have had an array of enthusiastic students seeking to broaden their research knowledge in the treatment of diseases.

This the forty-fourth edition of the Summer Student Research Program Abstracts summarizing research results generated by students, volunteers, and interns working thru this year's program. Since 1968 more than 3,500 students and volunteers have participated in this program. The Summer Student Research Program continues to provide a significant contribution to the training of our future clinicians and research scientists. It is the continued goal of this program to inspire the next generation of physicians and scientists.

We would like to thank the NJMS Faculty, et.al, who take time from their teaching and administrative responsibilities to mentor over the eight week period. We truly appreciate your continued support and exceptional commitment. It is also with pleasure that we thank the members of the faculty advisory committee…….for their assistance and commitment in developing the program guidelines, evaluating student abstracts, selection of student participants and your participation during our poster symposium. This program could not be as successful without your volunteerism! Many thanks to your for your kind consideration.

WE WOULD LIKE TO THANK THE FOLLOWING FACULTY FOR TAKING TIME TO MENTOR THE MEDICAL STUDENTS AND VOLUTEERS DURING OUR 2012 SUMMER STUDENT RESEARCH PROGRAM.

FACULTY ADVISORY COMMITTEE

Eric Altschuler, MD, Ph.D.
Assistant Professor
Physical Medicine & Rehabilitation

Deborah A. Lazzarino, Ph.D.
Assistant Dean for Research Administration
Office of Research & Sponsored Programs

Sheldon Lin, MD
Associate Professor
Department of Medicine

Purnima Bhanot, Ph.D.
Assistant Professor
Microbiology & Molecular Genetics

Diego Fraidenraich, PhD,
Assistant Professor
Cell Biology & Molecular Medicine

Carol Lutz, Ph.D.
Associate Professor
Biochemistry & Molecular Biology

Pranela Rameshwar, Ph.D.
Professor
Department of Medicine

Charles R. Spillert, Ph.D.
Associate Professor
Department of Surgery

Nila Dharan, MD
Assistant Professor
Department of Medicine

LECTURER:

Pranela Rameshwar, Ph.D.
Professor of Hematology, Department of Medicine

NJMS FACULTY MENTORS

Eric Altschuler, MD, Ph.D.
Assistant Professor
Physical Medicine & Rehabilitation

Soly Baredes, MD
Professor
Neurological Surgery

Susan Feldman, Ph.D.
Associate Professor
Department of Radiology

Chirag Gandhi, MD
Assistant Professor
Neurological Surgery

Betsy Barnes, Ph.D.
Associate Professor
Biochemistry & Molecular Biology

Purnima Bhanot, PhD.
Assistant Professor
Microbiology and Molecular Genetics

Ping-Hsin Chen, Ph.D.
Assistant Professor
Family Medicine

Melissa Rogers, Ph.D.
Associate Professor
Biochemistry & Molecular Biology

Sandra Scott, MD
Assistant Professor
Emergency Medicine

Ziad Sifri, MD
Associate Professor
Emergency Medicine

NJMS FACULTY MENTORS

Robert Heary, MD
Professor
Neurological Surgery

Sheldon Lin, MD
Associate Professor
Department of Medicine

James Liu, MD
Assistant Professor
Neurological Surgery

Patrick O'Connor
Associate Professor
Biochemistry & Molecular Biology

Alicia Mohr, MD
Associate Professor
Department of Surgery

Charles Prestigiacomo, MD
Professor & Chair
Neurological Surgery

Charles Spillert, Ph.D.
Associate Professor
Department of Surgery

Stella Elkabes, Ph.D.
Associate Professor
Neurological Surgery

Misun Park, Ph.D.
Assistant Professor
Cell Biology & Molecular Medicine

Francis Patterson, MD
Associate Professor
Department of Orthopaedics

Lizhao Wu, Ph.D.
Assistant Professor
Microbiology & Molecular Genetics

Charles Spillert, MD
Associate Professor
Department of Surgery

Ellen Townes-Anderson, Ph.D.
Professor
Neurology & Neurosciences

Yongkyu Park, Ph.D.
Adjunct Assistant Professor
Cell Biology & Molecular Medicine

Chaoyang Xue, Ph.D.
Assistant Professor
PHRI

Anna Barrett, MD
Professor
Physical Medicine & Rehabilitation

Robert Ledeen, Ph.D.
Professor
Neurosciences

Stanley Weiss, MD
Professor
Preventive Medicine & Community Health

Padmini Salgame, Ph.D.
Professor
Department of Medicine

John Capo, MD
Professor
Department of Orthopaedics

JUDGES FOR POSTER COMPETITION

Joel Freundlich, Ph.D.
Assistant Professor
Pharmacology & Physiology

Raymond Birge, Ph.D.
Professor
Biochemistry & Molecular Biology

Nasrin Ghesani, Ph.D.
Assistant Professor
Microbiology & Molecular Genetics

Hong Li, Ph.D.
Associate Professor
Biochemistry & Molecular Biology

Cheryl Kennedy, MD
Associate Professor
Department of Psychiatry

Deborah A. Lazzarino, Ph.D.
Assistant Dean for Research Administration
Office of Research & Sponsored Programs

Vivian Bellofatto, Ph.D.
Professor
Microbiology & Molecular Genetics

Elizabeth Moran, Ph.D.
Professor
Biochemistry & Molecular Biology

Nancy Connell, Ph.D.
Professor
Department of Medicine

Luis Ulloa, Ph.D., MS
Associate Professor
Department of Surgery

Sheldon Goldstein, MD
Associate Professor
Department of Anesthesiology

INTRODUCTION

The Summer Student Research Program provides an eight-week research experience for the New Jersey first-second year medical students, as well as undergraduate students enrolled in our combined BS/MD seven-year program. Students are required to participate in research activities in a basic science or clinical laboratory. On many occasions this has been the students first research experience. Participation allows students and volunteers to develop a close working relationship with their mentor.

After completing eight weeks of research in the respective laboratories, students present their research projects at the Summer Student Research Poster Symposium held in early August. At the symposium students are interviewed and required to explain the results displayed in their poster presentation. The abstracts preceding is a reflection of the commitment, dedication and enthusiasm of every student who participated in the Summer Student Research Program and students who presented at the 2012 Poster Symposium.

Congratulations to all the students and volunteers enrolled in the 2012 Summer Student Research Program! All the best and my you have continued success in your future endeavors!

Congratulations to Ms. Bailey Su the winner of the 2012 Summer Student Research Poster Competition!

THE MECHANISM OF ECHINOCANDIN DRUG RESISTANCE IN CRYPTOCOCCUS NEOFORMANS

GREGORY BAKER, CHAOYANG XUE, PH.D
DEPARTMENT OF MICRIOLOGY AND MOLECULAR GENETICS

OBJECTIVE:

Cryptococcus neoformans is an opportunistic yeast pathogen that leads to significant morbidity and mortality in immunocompromised individuals. Most notably it is the causative agent of the often fatal cryptococcal meningitis.
The course of treatment for cryptococcosis is limited. Currently an acute infection is treated with amphoterocin B or azoles in combination with 5-flucytosine. However, this course of treatment is not ideal. Amphoterocin B binds fungal as well as human sterols, thus it has many toxic side effects. Azoles, though better tolerated, are fungistatic rather than fungicidal and require a lifetime regimen of the drug. Additionally, increasing resistance of *C. neoformans* to 5-flucytosine is emerging which may render the drug ineffective. Lifelong courses of the drug in patients will only hasten this development. New and more efficacious treatments are needed to combat cryptococcosis.

The echinocandin class of drugs is a relatively new class of drugs that target (1,3)-b-glucan synthase, an enzyme that is both present and essential in *C. neoformans*. Despite this, *C. neoformans* is resistant to echinocandin treatment. It is not currently understood why the efficacy of echinocandin therapy in *C. neoformans* is limited.

Using a high-volume, systematic screen we intend to identify mutants sensitive to caspofungin, an echinocandin drug. A mutant library was created through co-culture of *C. neoformans* and *Agrobacterium tumefaciens*. *A. tumefaciens* randomly inserts T-DNA sequences containing a NAT resistant marker into the genome of the targeted organism. This random insertion may disrupt any of the ~6,500 genes present in *C. neoformans*. Therefore, we may generate a mutant strain of any of the non-essential genes in *C. neoformans*. After screening over 7,000 transformants, we have identified three sensitive mutants and through genotypic analysis identified the genes responsible for the observed increase in caspofungin sensitivity. Here we seek to provide a preliminary mechanism of drug resistance.

METHODS:

Strains and Media – A total of four mutant libraries were created from *Cryptococcus neoformans* var. *grubii* (serotype A) strain H99 and *C. neoformans* var. neoformans (serotype D) strain JEC21. In all growth assays transformants were grown in nutrient rich yeast extract peptone dextrose (YPD) media at 30° C. After measurements were taken, cultures were stored at 4° C.

Generation of *Agrobacterium* mediated mutagenesis library - Random mutagenesis library was created using strains *C. neoformans* var. *grubii* H99 and *Agrobacterium tumefaciens* EHA 105. Cells were grown in various fungal to bacterial cell ratios. After 48 hours, cultures were transferred to YPD with NAT and cefotaxime to select for *C. neoformans* strains with T-DNA insertions. Cells that grew on the selective media were transferred to 96 well plates and grown to saturation for further screening.

Library Screening – 96 well plates were prepared with 200ml YPD per well. 5 mL of saturated mutagenesis libraries stored at -80 °C were inoculated into each of the wells and incubated at 30°C. Growth in the absence of drug was determined by measuring the optical density at wavelength 600 nm (OD 600) every 24 hours for a total of 72 hours. Once cultures were saturated, transformants were screened for sensitivity to 8 mg/mL of caspofungin. 96 well plates were prepared with 200 ml YPD + 8 mg/mL of caspofungin. 5 mL of saturated cultures were inoculated into the corresponding wells. The OD600 was measured every 24 hours and growth in the presence of drug was compared to growth in YPD only. Transformants identified as having an increased sensitivity to drug compared to the wild type were selected for re-screening. After three screenings, sensitive mutants were selected for serial dilution study on agar plates. A total of four libraries were screened totaling 7,200 transformants.

Serial Dilution Study - Overnight cultures of transformants identified as sensitive to caspofungin were incubated at 30 °C and shaken at 220rpm. Cultures were spun down and washed with water. Their OD600 was measured. All cultures were diluted to a standardized OD600 of 1.000. 10 times serial dilutions were prepared and cultures were inoculated at four concentrations of caspofungin in YPD agar (0, 4, 8 and 16 mg/mL)

Co-segregation Assay - Isolates identified as sensitive to caspofungin and generated with H99α as a background were mated with strain KN99a. Mating was performed on two types of agar (MS and V8 agar). Cultures were prepared on YPD agar and incubated for 72 hours. After 72 hours cells from each culture were mixed and inoculated on MS and V8 media. Plates were incubated at 22.5°C in the dark for 10 days. After 10 days, spores were dissected and prepared on YPD + NAT plates and incubated at 30°C for 3 days. 30 colonies were selected from the YPD + NAT plates and transferred to new YPD + NAT plates. Cultures were mated with strain H99α and spores with the mating type a were selected for further study. Phenotypic and genotypic analysis was performed on the F1 progeny in the same manner as all other transformants.

Genotypic Analysis: Inverse PCR and Gene Identification - Transformants most sensitive to caspofungin were selected for genomic DNA extraction. Genomic DNA was prepared and digested with ClaI, NcoI, NdeI, BglII and XhoI for a total of five reactions. Digested fragments were self ligated with T4 DNA ligase, the flanking regions of the NAT insert were amplified and their sequences determined. The location of T-DNA insertion and subsequent gene disruption was determined using BLAST analysis of sequencing results with the *C. neoformans* genome database of the Broad Institute.

SUMMARY:

Library Screen - The initial high volume library screen for sensitivity to caspofungin at 8 mg/mL identified 106 transformants as sensitive to caspofungin.

Serial Dilution Study - All 106 transformants identified as more sensitive to caspofungin than wild type were studied using 10 times serial dilutions. From this study three transformants were selected as the most sensitive to caspofungin.

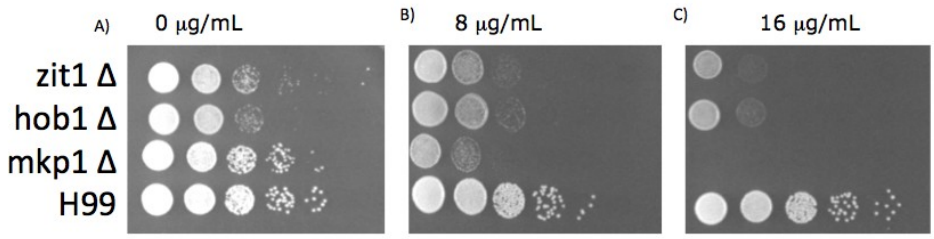

Figure 1 – Serial Dilutions at Three Caspofungin Concentrations (48 hours) Mutant mkp1D is hypersensitive to caspofungin while mutants zit1D and hob1D demonstrate increased sensitivity.

Co-segregation assay – After mating and selecting of appropriate progeny we observed that all of the offspring demonstrate a similar sensitivity to caspofungin. Genotypic analysis demonstrated the same disrupted genes as the parental strain.

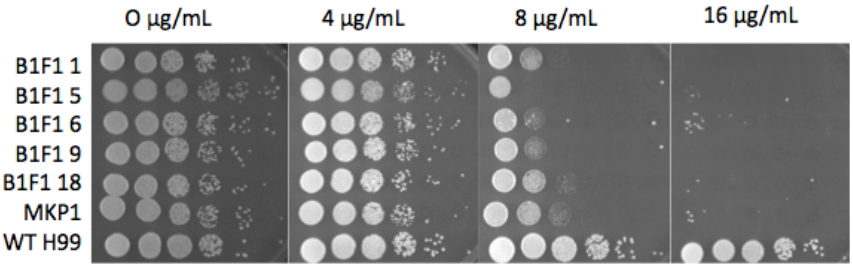

Figure 2 – 10X Serial Dilutions On Progeny from Co-segregation Assay

Genotypic Analysis – The method of genomic DNA extraction, digestion, self ligation, inverse PCR and subsequent sequencing identified four mutated genes in the three mutants. In hob1D a gene located on the first chromosome is disrupted. This gene is involved in endo and exocytosis. The zit1D mutant has a gene encoding a protein involved in zinc ion transport disrupted. Two genes are disrupted in mutant mkp1D. One gene is located on chromosome 13 and encodes a MAP kinase phosphatase (CNAG_03893). The other gene is located on chromosome 2 and encodes a transcriptional regulator (CNAG_06465).

Growth Assay - The growth of the three mutants are inhibited at a caspofungin concentration of 8 mg/mL while wild type H99 is not.

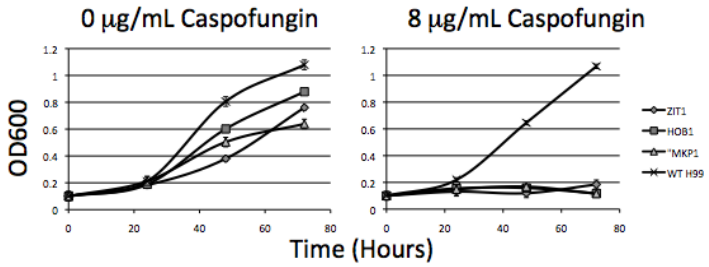

Figure 3 – Growth assay in YPD liquid medium containing *0* mg/mL and 8 mg/mL caspofungin respectively

Melanin Production - Mutants mkp1D, hob1D and zit1D were grown on niger seed agar media and incubated at 30°C and 37°C to observe melanin formation. There is no difference in melanin formation between mutant mkp1D and wild type H99. Both hob1D and zit1D showed significant melanin defect at 30° C and 37°C.

Capsule Production - Samples were inoculated on DME media and incubated at 30°C to induce capsule formation. Samples were observed with an India Ink stain. The MKP1 mutant produces large capsules. HOB 1 and ZIT 1 produce smaller capsules.

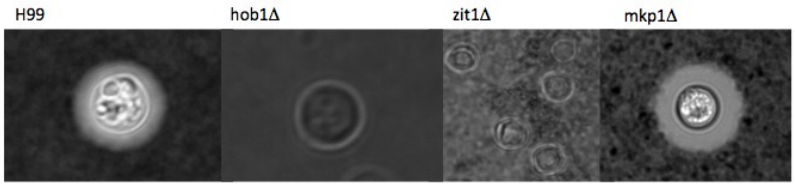

Figure 4 – India Ink Stain to visualize polysaccharide capsule

CONCLUSION:

As we expected, the mechanism of echinocandin drug resistance in *C. neoformans* appears complex, involving several different genes. The HOB1 gene is involved in endo and exocytosis while the ZIT1 gene encodes a zinc ion transporter. We hypothesize that this is significant in that it allows *C. neoformans* to rapidly remove and isolate echinocandin drugs from their drug target (1,3) b-glucan synthase. A clean gene knockout will need to be performed to confirm that the observed increase in drug sensitivity is in fact due to the genes disrupted by the T-DNA NAT insert.

The disrupted genes in the MKP1 mutant appear to be more complex. The co-segregation assay demonstrates that the observed increase in sensitivity is in fact due to a disruption of genomic information in *C. neoformans*. However, the results we have thus far suggest that either two insertions disrupted two separate genes or that a chromosomal rearrangement has occurred. The disrupted genes are a MAP kinase phosphatase and a transcriptional regulator. Further study will need to be done to determine the exact function of the transcriptional regulator as well as determine the number of NAT insertions that occurred. Despite the ambiguity at this point in time of what is occurring genomically, the phenotype of this mutant is very promising. It displays hypersensitivity to caspofungin at 8 mg/mL, still maintains the typical virulence factors of *C. neoformans* and passes this sensitivity to its progeny when it is mated with another strain. While there is much that remains to be known, significant strides have been made in the understanding of the mechanism of drug resistance in *C. neoformans* and we hope to gain a clearer understanding in the near future.

REFERENCES:

Denning, D.W. (2003). "Echinocandin antifungal drugs." The Lancet 362:1142-1151.

Feldmesser, M. et. Al (2000) "The Effect of the Echinocandin Analogue Caspofungin on Cell Wall Glucan Synthesis by *Cryptococcis neoformans*" Journal of Infectious Disease 82: 1791-1795

Idnurm, A. et al. (2004). "*Cryptococcus neoformans* Virulence Gene Discovery through Insertional Mutagenesis." Eukaryotic Cell 3(2): 420 – 429.

Malagie, M.A. et al (2005) "*Cryptococcus neoformans Resistance to Echinocandins: (1,3)-Glucan* Synthase Activity Is Sensitive to Echinocandins" Antimicrobial Agents and Chemotherapy 49(7): 2851-2856

Park, B. J. et al. (2009) "Estimation of the current global burden of cryptococcal meningitis among persons living with
HIV/AIDS" AIDS 23: 525-530

Perlin, D.S. (2011) "Current perspectives on echinocandin class drugs" Future Microbiology 6(4): 441-457

AUF1 BINDING OF THE ULTRA-CONSERVED SEQUENCE IN THE 3' UNTRANSLATED REGION ON BMP-2 MRNA

SANDRA CHESONI, MELISSA ROGERS, PH.D.
DEPARTMENT OF BIOCHEMISTRY & MOLECULAR BIOLOGY

OBJECTIVE:

To investigate the association of AUF1 with the ultra-conserved sequence (USC) at the AU-rich sequence ARE8/9 of Bmp2 mRNA

BACKGROUND:

Bone morphogenetic protein 2 (BMP2) is a multi-functional growth factor with essential roles in cardiac, neural, cartilage, and bone development. BMP2 dysregulation is linked to pathophysiological conditions such as obesity, cancer, and vascular diseases. The clinical potential of modulating BMP2 expression in these conditions has yet to be fully explored and may help pioneer a new generation of therapeutics. The Bmp2 transcript contains an ultra-conserved sequence (UCS) within the 3'UTR. The UCS functions as a *cis*-acting repressor in coronary vasculature and deletion of the UCS is sufficient to abrogate repression. The UCS bears an A+U rich element (ARE) known to bind HuR, an ARE binding protein (AUBP). HuR induces Bmp2 mRNA levels. Data from an *in vitro* affinity selection assay shows AUF1, another AUBP also binds the Bmp2 transcript. In contrast to HuR, AUF1 promotes degradation of ARE containing transcripts. AUF1 has been implicated in cardiovascular disease. For example, AUF1 interacts with the β2-adrenergic receptor (β2-AR) messenger in an ARE dependent manner. AUF1 is upregulated in congestive heart failure (CHF), concomitant with β2-AR) messenger downregulation. Elevated levels of AUF1 may contribute to CHF by downregulating β2-AR mRNA and subsequently reducing levels of β2-AR protein. The role of AUF1 in coronary vasculature pathogenesis in not known. We therefore want to explore the *in vivo* interaction between AUF1 and the Bmp2 mRNA and determine the role the UCS plays in AUF1
binding kinetics.

METHODS:

Cell lysates used were from: A549 - a lung cancer cell line that expresses BMP-2, BEAS-2B - a non-transformed lung cell that does not express BMP-2, BEAS-2B cells stably transfected with Bmp2 reporter mRNAs that bear the UCS, lack the UCS, or with a mutation in the AUBP binding site. Cell lysates were pre-cleared with rabbit non-immune serum and magnetic Dynabeads coupled to protein A. Fresh beads were coated with anti-AUF1 or rabbit non-immune serum. Next pre-cleared lysates were incubated with anti-AUF1 coated or rabbit non-immune serum coated beads. To isolate AUF1-associated mRNAs, proteins were digested with proteinase K and DNA with DNase 1, following these treatments mRNA was purified by phenol-chloroform extraction. Association of natural Bmp2 mRNA or reporter mRNAs that
bear the UCS with AUF1 was assayed by reverse transcription.

Results:

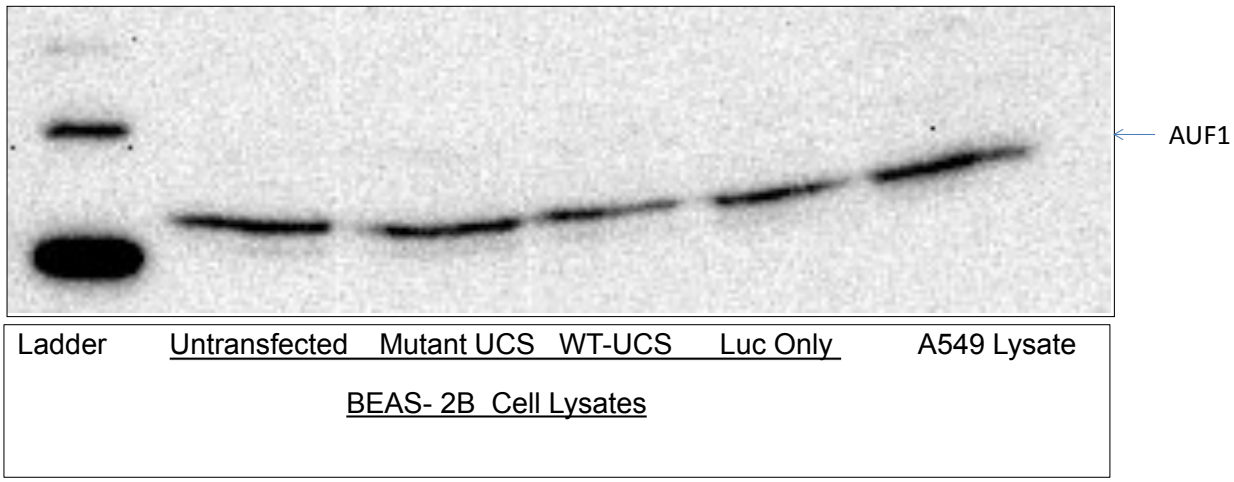

Figure 1: AUF1 is expressed in A549 and BEAS-2B cells.

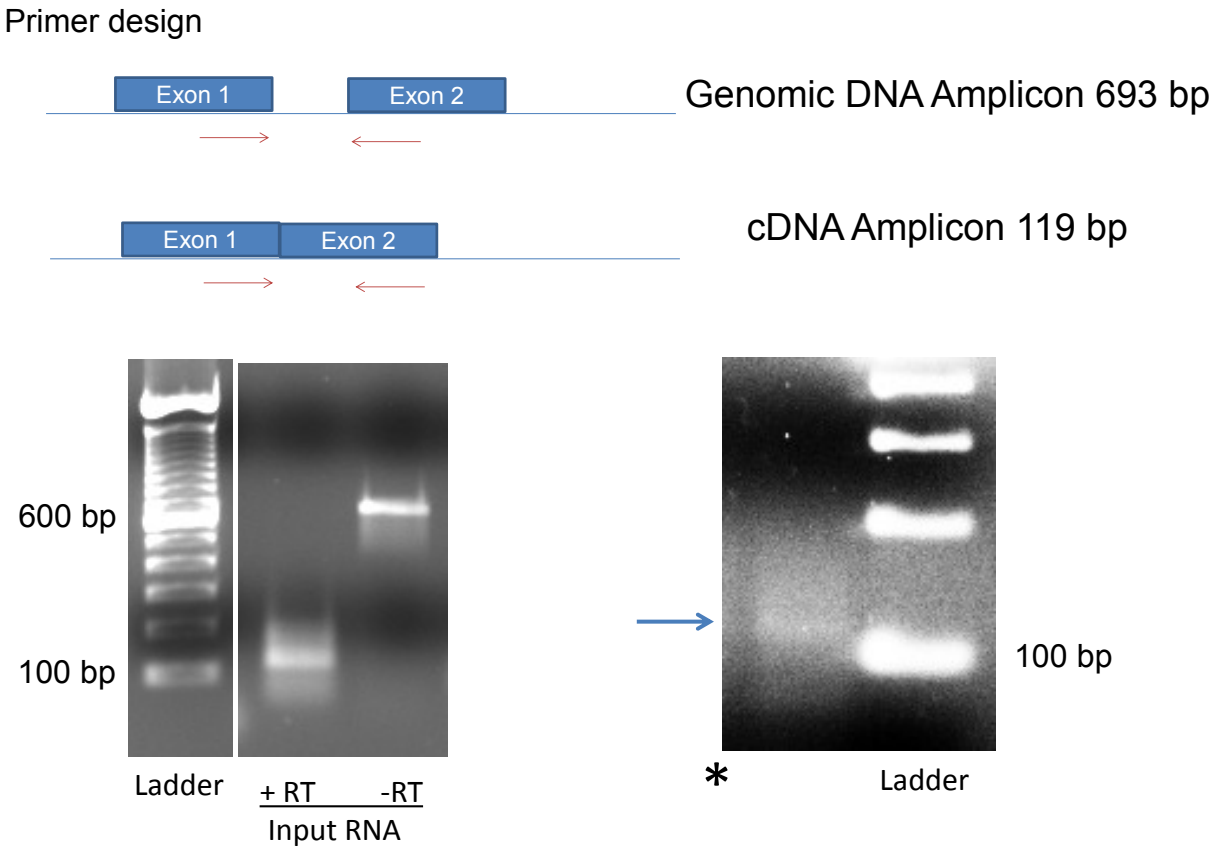

Figure 2: Amplification of Bmp2 Reporter Transcript from Beas-2B cells transfected with CMV-BMP2-UCS

Conclusions

Our results suggest that AUF1 associates with mRNAs bearing the Bmp2 UCS in vivo.

Future Experiments

Optimization of qRT-PCR conditions for amplification of AUF1 associated mRNAs

Knockdown of AUF1 by stable transfection of the AUF1 shRNA-expressing plasmid

Assessment of AUF1 levels in knockdown cells by western blot analysis

Assessment of Bmp2 mRNA levels in an AUF1 knockdown background

Assessment of BMP2 protein levels in an AUF1 knockdown background

Mutation of Mir-633 binding site and/or AUBP binding site

Assessment of BMP-2 mRNA and protein levels in single vs. double mutations

INTIMATE PARTNER VIOLENCE DURING PREGNANCY IN ILLITERATE IMMIGRANT WOMEN: BIRTH OUTCOMES AND DEPRESSION

ANH-CHI DO, PING-HSIN CHEN, PH.D.
DEPARTMENT OF FAMILY MEDICINE

BACKGROUND:

Intimate partner violence (IPV) during pregnancy affects 4-8% of pregnant women each year. The American Congress of Obstetricians and Gynecologists recommends that IPV screening should occur during the first pre-natal visit, once during each trimester, and at the post-partum visit. Screening for IPV in immigrants can be difficult due to language and cultural barriers. Pregnant women who are immigrants are therefore at risk of being under-screened, and consequently not receiving adequate prenatal care as related to IPV during pregnancy.

Studies have found that women who are victims of both psychological aggression and physical abuse have higher levels of depression during pregnancy than non-victims. In addition, IPV during pregnancy is associated with unplanned pregnancy, low birth outcomes, including increased risk of preterm delivery, low birth weight, and child intensive care. '

OBJECTIVE:

The aim of the study was to examine the differences in depressive symptoms and birth outcomes between illiterate immigrant pregnant women who are victims of IPV and those who are non-victims. It is hypothesized that victims of IPV will have increased depressive symptoms and lower birth outcomes, including increased high risk pregnancies, increased preterm deliveries, lower birth weights, and increased child intensive care.

METHODS:

This was a retrospective cohort study that examined IPV during pregnancy among illiterate immigrant women. The target population was pregnant women seen at the University Hospital (UH) prenatal clinic who were given the ICD-9 code of 315 for reading disability, who were born outside of the US, and who gave birth at the UH. A total of 200 medical charts were reviewed. Women with mental or congenital disabilities (n=4) were excluded from the study to ensure that the study population only included women who were illiterate due to language or education barriers (n=196). Pregnant women were screened for IPV using the HITS (Hurt, Insult, Threaten, Scream) tool. The standard cutoff score of >10 and

Rodriguez M, Shoultz J, Richardson E. Intimate Partner Violence Screening and Pregnant Latinas. Violence and Victims 2009;24:520-532.

Martin SL, Li Y, Casanueva C, Harris-Britt A, Kupper LL, Suzanne C. Intimate partner Violence and Women's Depression Before and During Pregnancy. Violence Against Women 2006;12:221-239.

Pallitto CC, Campbell JC, O'Campo P. Is Intimate Partner Violence Associated with Unintended Pregnancy? A Review of the Literature. Trauma, Violence, & Abuse 2005;6:216-235.

Coker AL, Sanderson M, Dong B. Partner violence during pregnancy and risk of adverse pregnancy outcomes. Paediatric and Perinatal Epidemiology 2004;18:260-9.

documentation of IPV was used to determine victim status in our study. Depression was defined as a score of ≥10 on the Edinburgh Postnatal Depression Scale (EPDS) at the antepartum or postpartum visit. A gestational age of less than 37 weeks was recorded as preterm delivery. Low birth weight was defined as < 2,500grams.

SUMMARY:

14.5% of the women in this study were victims of IPV (n=27). Victims and non-victims did not differ significantly in frequencies of high risk pregnancy (23.1% vs. 26.6%, p>0.05), preterm delivery (7.4% vs. 10.1%, p>0.05), low birth weight (12% vs. 4.8%, p>0.05), or neonatal transfer to intensive care (3.7% vs. 3.1%, p>0.05).

Victims of IPV were more likely to have unplanned pregnancies (100% vs. 71.4%, p=.021) and a history of child abuse (11.1% vs. 1.9%, p=.041) when compared to non-victims. IPV victims also had a significantly higher frequency of antepartum and/or postpartum depressive symptoms (50% vs. 25%, p=0.014).

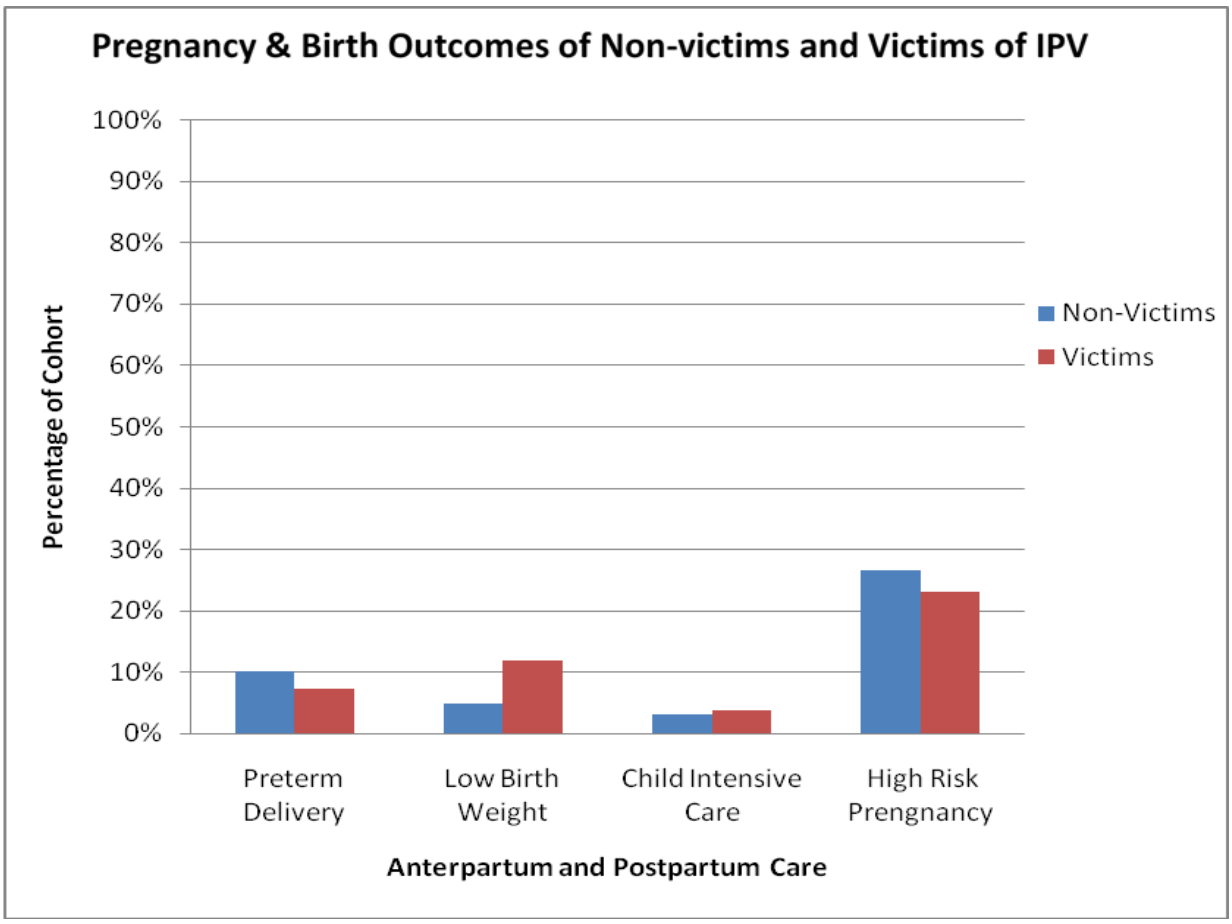

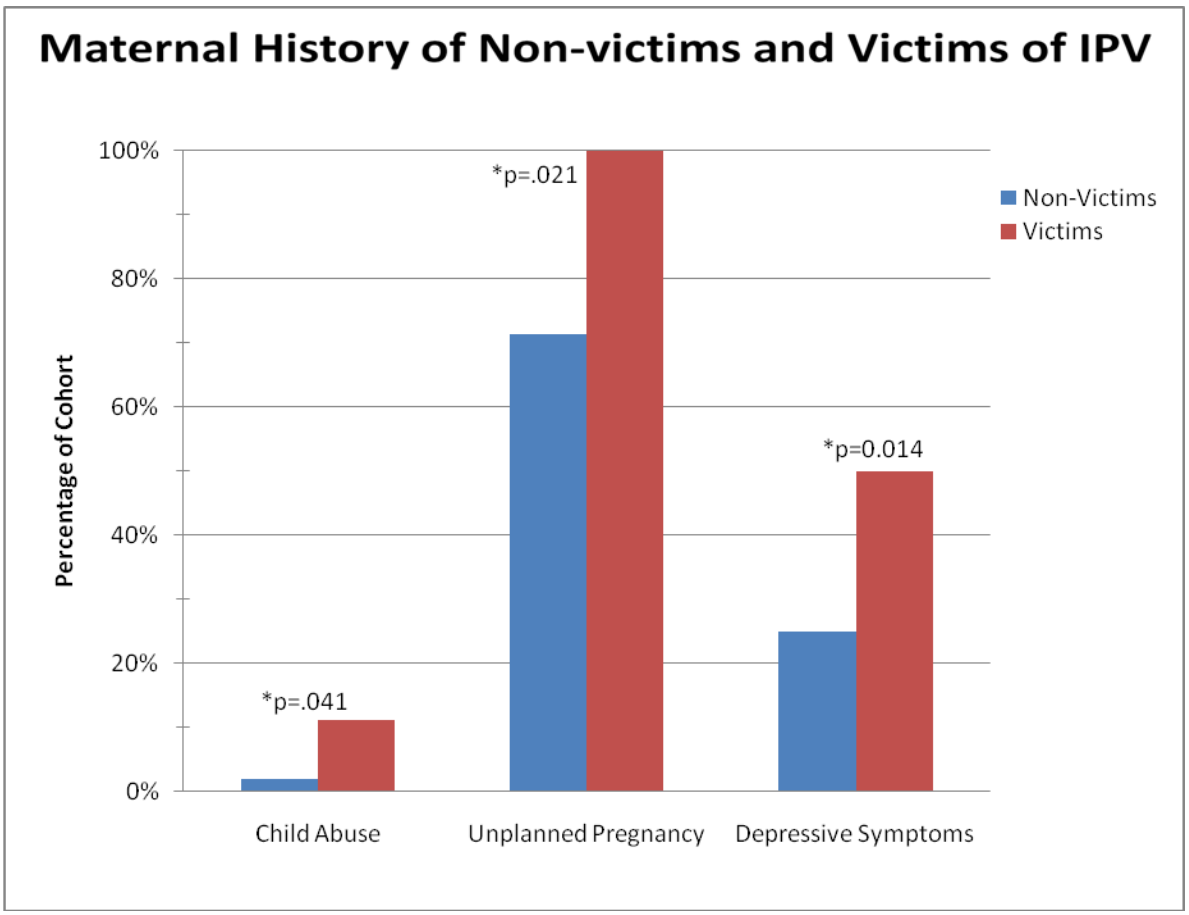

CONCLUSION:

Although previous studies have found less favorable birth outcomes in women who are victims of IPV during pregnancy, our data did not show a significant difference in birth outcomes between victims and non-victims of IPV during pregnancy.

Within our cohort, all women who were victims of IPV had unplanned pregnancies, while the percentage of unplanned pregnancies in non-victims was significantly lower. Unplanned pregnancies have been previously associated with increased risk of IPV. Victims of IPV were significantly more likely to suffer from depressive symptoms than non-victims. More research is needed to assess whether unplanned pregnancy is a confounding variable that affects the link between IPV and depression.

Our data also showed that a significantly larger percentage of victims had a history of child abuse compared to non-victims. However, due to missing data on this variable, child abuse may be underreported for both victims and non-victims.

Health care providers should continue to screen for IPV and identify pregnant women who are victims, especially those who are illiterate immigrants. Although communication may be difficult in such cases, interventions should be designed to reduce IPV and depressive symptoms.

IN-HOSPITAL MORBIDITY AND SPATIAL NEGLECT AFTER RIGHT BRAIN STROKE

ANTHONY DOSS, A.M. BARRETT, MD*, KRISTEN K. MAUL **
DEPARTMENT OF PHYSICAL MEDICINE & REHABILITATION*
&
KESSLER FOUNDATION RESEARCH CENTER, WEST ORANGE, NJ**

PARTICIPATION DESCRIPTION

In this project, my involvement was reviewing the 4610 charts of patients admitted to the Kessler Institute for Rehabilitation over a four year period. I isolated variables from the charts and performed various data analyses in an attempt to represent the data and statistical analysis in a clear way. I also observed several screenings of subjects and wrote descriptions of the tests used in an attempt to better analyze and re-structure the data. I also researched prior studies related to the individual measures of stroke morbidity in an attempt to take a closer, more qualitative look at which ones may be related to spatial neglect.

[1]Kessler Foundation Research Center, West Orange NJ;
[2]Meharry Medical College, Nashville Tennessee;
[3]Kessler Institute for Rehabilitation, West Orange, NJ;
[4]University of Medicine and Dentistry of New Jersey – New Jersey Medical School, Newark, NJ

Spatial neglect commonly occurs after right hemisphere lesions[1] and manifests as lateralized bias in attention and action, impairing the ability to respond or orient to stimuli on the contralesional body, causing functional disability.[2] Spatial neglect is associated with poor stroke outcome and increased length of hospital stay[3,4,5]. This study explores the relationship between administrative indicators of stroke morbidity and presence of spatial neglect.

OBJECTIVE:

determine the association between signs and symptoms of spatial neglect and clinical indicators of rehabilitation outcome following stroke.
We predict that compared to the average stroke population, stroke patients with neglect will have:

Longer Length of Stay

Lower rehabilitation efficiency during hospitalization (FIM change / day; Long et al., 1994)

Increased incidence of medical complications resulting in transfer back to acute care settings

Lower level of independence at discharge (home vs. acute- sub-acute facility)

METHODS:

Design:

Ongoing chart review during the period of 6/12/2008 to 6/01/2012 resulted in a total of 4610 records with stroke diagnosis, and a sample of 177 individuals completing a comprehensive assessment for spatial neglect.

PARTICIPANTS:

The sampled population included only patients who had suffered single, right hemisphere stroke. These patients underwent a comprehensive pre-screening for spatial neglect and eligibility for treatment studies, including the Behavioral Inattention Test (BIT), and tasks designed to screen patients for unilateral visual neglect deficits. Patients met the BIT criterion for neglect with a score $\leq$ 129 of 146. All procedures were conducted after informed consent and with local IRB approval.

SUMMARY:

Length of Stay: Neglect patients stayed longer in acute rehabilitation (M = 28.2 days; SD = 10.1) than average stroke rehabilitation candidates (M = 19.6 days; SD = 12.0), U test: z = 8.5, p = <0.01.

Discharge destination: Fewer individuals with neglect went home following acute rehabilitation (39%) compared to the average stroke rehabilitation candidates (52%), p<0.01, Fisher's Exact Test, one-tailed. Patients with neglect were more-likely to be discharged to sub-acute settings than other stroke survivors (41% versus 27% ; p<0.01, FET one-tailed).

Rehabilitation efficiency: Neglect patients had lower rehabilitation efficiency than average stroke candidates (M= 0.86 point; SD = 0.72 vs. M = 1.14 points; SD = 1.5; z= 3.2, p = <0.01).

Acute Care Transfers: Although more neglect patients (12%; non-neglect patients, 2%) were transferred to acute care during acute rehabilitation, this did not reach significance (p=0.09)

CONCLUSION:

Stroke patients with spatial neglect have poorer outcomes on several administrative rehabilitation outcome measures of function and independence. Identifying neglect early in stroke rehabilitation and providing appropriate treatment during acute rehabilitation may improve longer-term outcomes for stroke patients suffering from spatial neglect.

References

1. Buxbaum, L.J., M.K. Ferraro, T. Veramonti, et al. 2004. Hemispatial neglect: subtypes, neuroanatomy, and disability. *Neurology.* 62:749-756

2. Heilman, K.M., R.T. Watson & E. Valenstein. 2003. Neglect and related disorders. In *Clinica Neuropsychology.* K.M. Heilman & E. Valenstein, Eds.:296-346. Oxford University Press. New York, NY

3. Barrett, A.M. & Burkholder, S., 2006. Monocular patching in subjects with right-hemisphere stroke affects perceptual-attentional bias. J Rehabil Res Dev 43: 337-346.

4. Cherney LR, Halper AS, Kwasnica CM, Harvey RL, Zhang M. 2001. Recovery of Functional Status After Right Hemisphere Stroke: Relationship with Unilateral Neglect. *Arch Phys Med Rehabil*. Mar; 82: 322-8

5. Jehkonen M., M. Laihosalo & J.E. Kettunen. 2006. Impact of neglect on functional outcome after stroke: a review of methodological issues and recent research findings. *Restor. Neurol. Neurosci.* 24:209-215

TREATMENT OPTIONS FOR ACUTE BASILAR ARTERY OCCLUSION: A DECISION ANALYSIS

MICHAEL FASTIGGI,TANK, V., JETHWA, P., SIVARAJU, A., FASTIGGI, M., LANDER, M., DUFFIS, EJ., PRESTIGIACOMO, C., GANDHI, C.
DEPARTMENT OF NEUROSURGERY

BACKGROUND AND PURPOSE:

Acute basilar artery occlusion (BAO) is a medical emergency that often results in poor clinical outcome, including locked-in syndrome or death. Therefore, timely recanalization of BAO is of paramount importance. Currently, there is no "gold standard" treatment for acute BAO. The purpose of this study was to perform a decision analysis to determine the optimal treatment modality for BAO.

METHODS:

A decision analysis model was created using TreeAge Pro Suite 2012 (See Figure 1). The treatment options were "Conservative", "IV tPA", "IA tPA", or "Thrombectomy". Studies specifically pertaining to treatment of acute BAO with the one or more of the above treatment options were analyzed to obtain values for the input parameters. Statistical analysis of the data was performed using the TreeAge software, including 1-way and 2-way sensitivity analyses, as well as Monte Carlo simulation.

RESULTS:

In the base case scenario "IA tPA" and "Thrombectomy" had the highest expected values (0.38 and 0.37 quality-adjusted life years (QALY), respectively), followed by "IV tPA" (0.32 QALY), "Conservative" (0.26 QALY). The results of 1-way sensitivity analysis showed that "Thrombectomy" became the optimal strategy if the recanalization rate was greater than 88.5% or the symptomatic hemorrhage rate was less than 27.4%. The results of the 10,000 iteration Monte Carlo simulation showed that "IA tPA" was the optimal strategy in 59.8% of cases, followed by "Thrombectomy" in 38.5%, and "IV tPA" in 1.7%.

CONCLUSION:

Acute BAO treatment with either thrombectomy or IA tPA increases the likelihood of better outcomes over IV tPA or conservative management.

Figure 1:

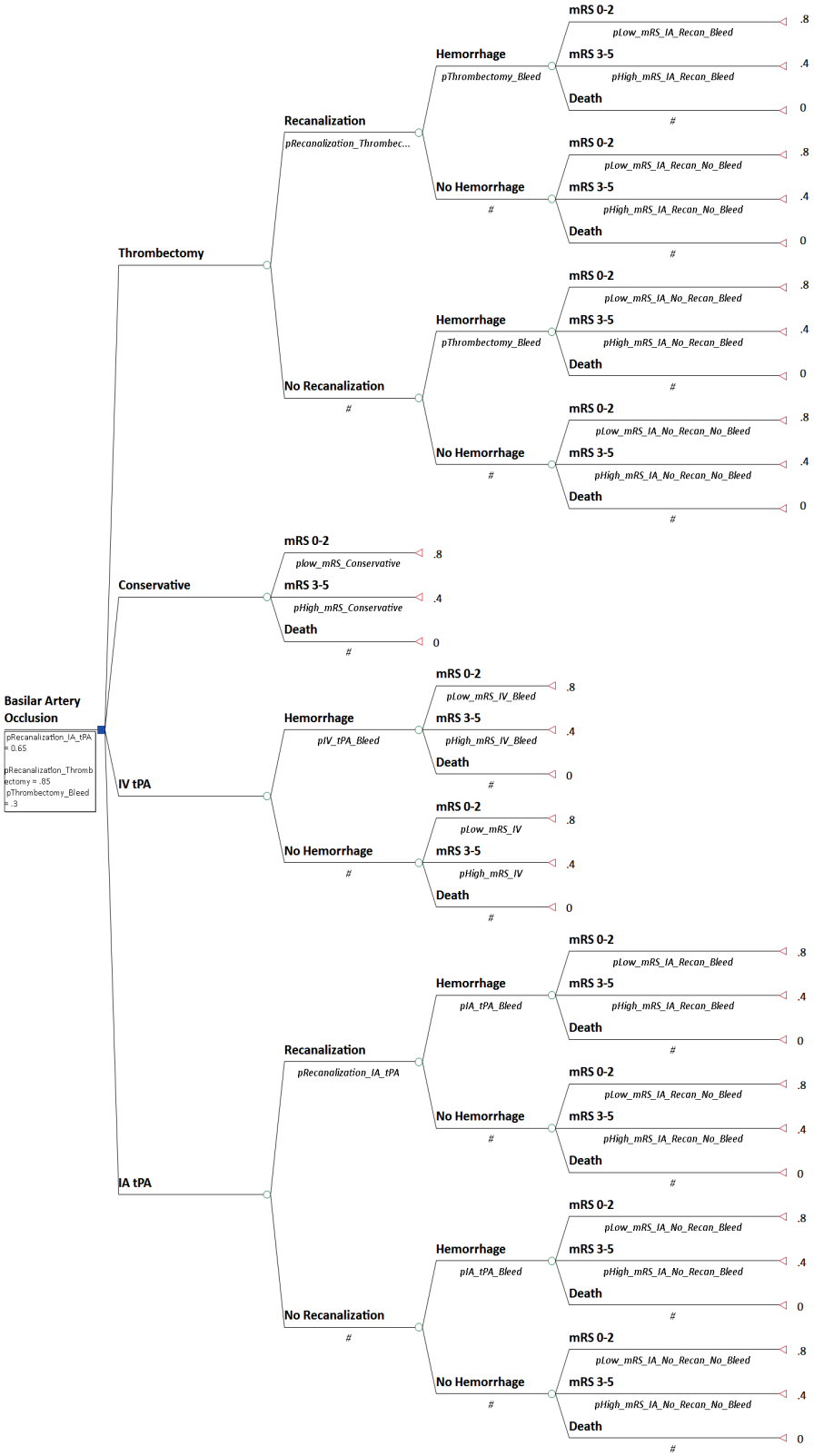
Basilar Artery Occlusion
pRecanalization_IA_tPA = 0.65
pRecanalization_Thrombectomy = .85
pThrombectomy_Bleed = .3
Thrombectomy
Recanalization
pRecanalization_Thrombec...
Hemorrhage
pThrombectomy_Bleed
mRS 0-2
pLow_mRS_IA_Recan_Bleed
.8
mRS 3-5
pHigh_mRS_IA_Recan_Bleed
.4
Death
0
#
No Hemorrhage
#
mRS 0-2
pLow_mRS_IA_Recan_No_Bleed
.8
mRS 3-5
pHigh_mRS_IA_Recan_No_Bleed
.4
Death
0
#
No Recanalization
#
Hemorrhage
pThrombectomy_Bleed
mRS 0-2
pLow_mRS_IA_No_Recan_Bleed
.8
mRS 3-5
pHigh_mRS_IA_No_Recan_Bleed
.4
Death
0
#
No Hemorrhage
#
mRS 0-2
pLow_mRS_IA_No_Recan_No_Bleed
.8
mRS 3-5
pHigh_mRS_IA_No_Recan_No_Bleed
.4
Death
0
#
Conservative
mRS 0-2
pLow_mRS_Conservative
.8
mRS 3-5
pHigh_mRS_Conservative
.4
Death
0
#
IV tPA
Hemorrhage
pIV_tPA_Bleed
mRS 0-2
pLow_mRS_IV_Bleed
.8
mRS 3-5
pHigh_mRS_IV_Bleed
.4
Death
0
#
No Hemorrhage
#
mRS 0-2
pLow_mRS_IV
.8
mRS 3-5
pHigh_mRS_IV
.4
Death
0
#
IA tPA
Recanalization
pRecanalization_IA_tPA
Hemorrhage
pIA_tPA_Bleed
mRS 0-2
pLow_mRS_IA_Recan_Bleed
.8
mRS 3-5
pHigh_mRS_IA_Recan_Bleed
.4
Death
0
#
No Hemorrhage
#
mRS 0-2
pLow_mRS_IA_Recan_No_Bleed
.8
mRS 3-5
pHigh_mRS_IA_Recan_No_Bleed
.4
Death
0
#
No Recanalization
#
Hemorrhage
pIA_tPA_Bleed
mRS 0-2
pLow_mRS_IA_No_Recan_Bleed
.8
mRS 3-5
pHigh_mRS_IA_No_Recan_Bleed
.4
Death
0
#
No Hemorrhage
#
mRS 0-2
pLow_mRS_IA_No_Recan_No_Bleed
.8
mRS 3-5
pHigh_mRS_IA_No_Recan_No_Bleed
.4
Death
0
#

CHARACTERIZATION OF B CELL AGGREGATES IN MURINE LUNGS DURING MYCOBACTERIUM TUBERCULOSIS INFECTION

ANDREW H. KIM, PADMINI SALGAME, PH.D, KAMLESH BHATT, PH.D.
DEPARTMENT OF MEDICINE

INTRODUCTION:

According to WHO statistics, in 2010 alone there were 8.8 million people worldwide that were infected with *Mycobacterium tuberculosis*, and a total of 1.4 million people succumbed to the disease. *Mycobacterium tuberculosis* can reside in most organs, however pulmonary tuberculosis is the form most commonly seen.

The defining characteristic of tuberculosis disease is the formation of granulomas that plays an important role in the containment of infection [1]. These granulomas consist of groups of different immune cells such as macrophages, T cells and B cells. One characteristic feature of granuloma in both humans and mouse models of the disease is the predominant presence of B cell aggregates that resemble B cell follicles found in secondary lymphoid organs. This characteristic of granulomas is interesting, seeing that B cells and antibodies were classically thought to contribute little towards protection against *Mtb*, with cell-mediated immunity playing the predominant role [2]. However, recent studies have shown that B cells are required for proper containment of bacilli in the lung, and can significantly moderate inflammatory progression during disease [3]. In addition, some of these ectopic B cell aggregates contain germinal center (GC) markers. This suggests that tertiary lymphogenesis is occurring in the lung in response to tuberculosis disease, and since ag-specific B cell maturation is known to occur in germinal centers of other lymphoid organs, these ectopic B cell follicles are likely contributing significantly in the host response to *Mtb* infection [3]. These studies suggest that B cells may have a more critical role during *Mtb* infection than was originally thought.

The objective of this study is to further characterize the role of these B cell aggregates in granuloma by viewing their architecture using immunohistochemical staining with CD20 antibody, a B cell marker, and peanut agglutinin (PNA), a lectin that is a germinal center marker of B cells. In addition, we aim to elucidate the clonal repertoire of these B cells by performing PCR analysis of genomic DNA extracted from lymphoid aggregates in the granuloma using laser capture microscopy (LCM).

METHODS:

MICE:

WT C57BL/6 mice were purchased from NCI.

INFECTION:

The virulent Erdman strain (Trudeau Institute, Saranac Lake, NY) of *M. tuberculosis* was obtained from a mouse lung, grown in culture, titrated, and stored in aliquots at -70°C. Before infection, aliquots were thawed and briefly sonicated. The In-TOX Products aerosolization apparatus was used to infect mice via the respiratory route.

ANALYSIS OF TISSUES:

Lungs were harvested from mice at indicated time points. The lungs were first perfused with PBS and the right middle lobe was fixed in 4% paraformaldehyde for 7 days and then paraffin embedded.

IMMUNOHISTOCHEMISTRY:

Immunohistochemical staining was performed on 5 μm FFPE lung tissue sections obtained from WT C56BL/6 mice 8 weeks post infection. The sections were first deparaffinized and hydrated. Antigen was exposed using the citrate buffer antigen retrieval method.

For PNA staining, sections were treated with 3% H_2O_2 to block endogenous peroxidase activity. The tissue was then incubated at room temperature (RT) with 1X PowerBlock (Biogenex) and avidin/biotin blocking solution (Vector) in order to reduce non-specific staining. Biotinylated PNA (Vector) was then added and incubated at RT for 1 hour at a concentration of 20 μg/mL. PNA diluted in 500mM galactose was used as a negative control. The tissue was subsequently incubated in streptavidin peroxidase (Biogenex) for 25 minutes and then labeled with diaminobenzidine substrate. Counterstain was performed
using Mayer's Hematoxylin (Sigma)

For CD20 staining, sections were treated with 0.3% H_2O_2 and the same blocking steps were performed as above. Sections were incubated with CD20 goat polyclonal IgG (Santa Cruz) or goat IgG isotype (Vector) for 1 hour at RT. Biotinylated goat IgG (Vector) was then added and left to incubate at RT for 45 minutes. Detection and labeling of the antibody and counterstain were then performed in the same manner as above.

DNA extraction and purification from Mtb infected mouse lungs FFPE lung tissue was obtained from *Mtb* infected mice 11 weeks post infection. The lung tissue was cut into 5 μm sections and placed onto microscope slides. The sections were deparaffinized and hydrated and subsequently stained with cresyl violet in order to visualize the granulomas. Three separate granuloma from three different WT infected mouse lung were excised using the Zeiss PALM Microlaser system and catapulted into tubes with adhesive caps (Zeiss). 25 μL of Proteinase K Extraction Solution (Pico Pure) was added into each tube and incubated inverted for 24 hours at 65°C. The proteinase K was inactivated via incubation at 95°C for 10 minutes. Protein was removed from samples using phenol:chloroform: isoamyl alcohol 25:24:1 (Sigma)

and an overnight ethanol precipitation was performed. Samples were then resuspended in 10μL of 1X TE buffer. DNA concentrations and 260/280 absorbance were quantified using the NanoDrop 1000 spectrophotometer. DNA was then sent out for PCR analysis to determine clonality.

Results:

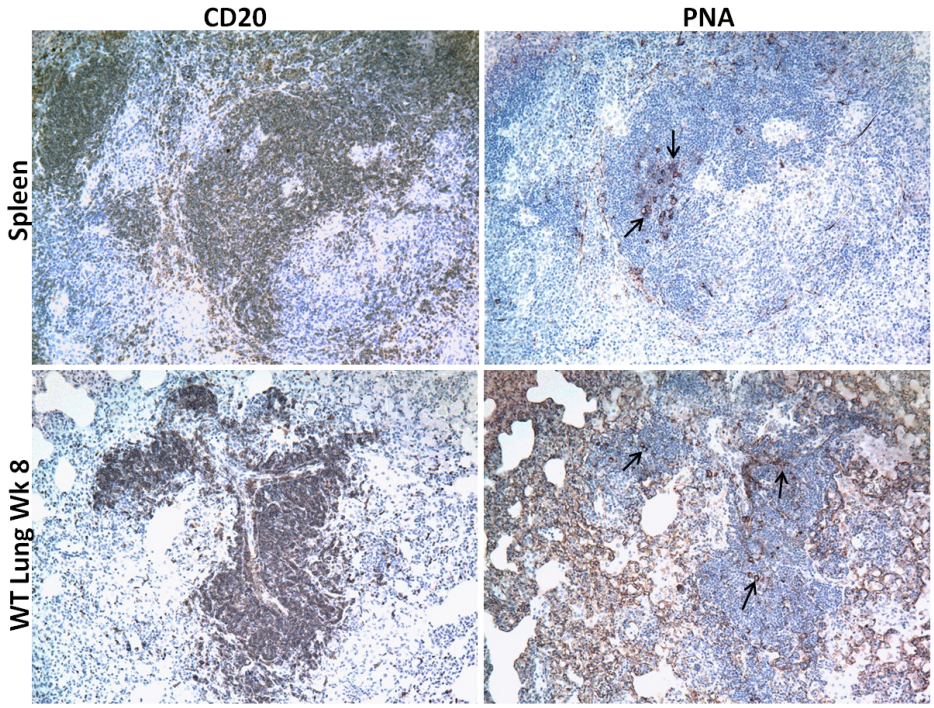

Fig. 1. Immunohistochemical detection of CD20+ and PNA+ B cells in formalin fixed paraffin embedded lung tissue obtained from WT C57BL/6 mice 8 weeks post infection. Serial sections were stained with the B cell marker CD20 and PNA, a GC marker. Spleen was used as a positive control to confirm proper staining. CD20+ B cell aggregates are seen making up the majority of the cells in the lung granuloma. Ectopic GC B cells can be seen scattered throughout the granuloma. CD20+ Bcells and PNA GC B cells: dark brown stain. Black arrows are pointing to areas of PNA staining. Magnification: 10x.

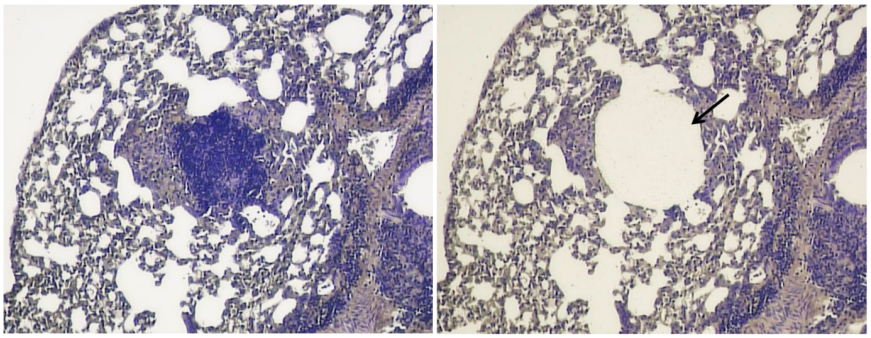

Fig. 2. Prior to and following LCM dissection of individual granuloma in the lungs of C57BL/6 mice 11 weeks post infection with *M. tuberculosis* Erdman. Lung sections were stained with cresyl violet in order to visualize granuloma. Locations of lymphocytic infiltration appear as dark, dense blue areas. The black arrow is pointing to the excised area. Magnification: 10x.

Table 1. DNA extraction and purification from granuloma excised from *M. tuberculosis* infected mice lung.

	Granuloma	260/280 before purification	Concentration before purification (ng/μL)	Total DNA before purification (ng)	260/280 after purification	Concentration after purification (ng/μL)	Total DNA after purification (ng)
Mouse 1	1	0.91	44.1	970	2.08	12.9	129
	2	0.88	43.9	878	2.12	10.4	104
	3	0.88	44.0	968	1.83	15.1	151
Mouse 2	1	0.92	44.8	941	2.13	9.0	90
	2	0.88	43.1	711	1.81	18.4	184
	3	0.89	44.2	906	2.25	7.7	77
Mouse 3	1	0.89	44.2	928	1.91	8.8	88
	2	0.88	44.5	979	1.94	8.8	88
	3	0.90	43.3	909	1.60	16.7	167

260/280 absorbance, concentration and total amount of DNA obtained prior to and following phenol/chloroform purification and ethanol precipitation. Three separate granuloma were excised from three individual WT C57BL/6 mice 11 weeks post infection with *M. tuberculosis* Erdman. Samples were in a 25 μL volume of Proteinase K solution before purification and were resuspended in 10 μL of TE buffer after purification. There was a significant increase in the 260/280 absorbance after protein was removed from samples, however there was also a significant loss of DNA.

Conclusion:

PNA and CD20 staining were successfully standardized, and the staining allowed us to view the presence of B cell aggregates and ectopic GCs in granuloma during chronic *Mycobacterium tuberculosis* infection. Optimization of granuloma isolation from *Mtb* infected mouse lungs using LCM was achieved, and an adequate amount of DNA was successfully extracted and purified from granuloma. The DNA is currently being analyzed to determine the clonality of the B cell clusters in the granuloma. The techniques that were optimized in this study will be used in future studies to investigate B cell specific gene expression from different time points using RNA extracted from granuloma excised from OCT lung sections.

References:

1. Flynn, J., and Chan, J., Immunology of tuberculosis. *Annu. Rev. Immunol.* 2001. **19**: 93-129
2. Tsai, M.C., Chakravarty, S., Zhu, G., Xu, J., Tanaka, K., Koch, C., Tufariello, J. *et al.*, Characterization of the tuberculous granuloma in murine and human lungs: cellular composition and relative tissue oxygen tension. *Cell. Microbiol.* 2006. **8**: 218-232.
3. Maglione P.J., Jiayong Xu and Chan, J. B cells moderate inflammatory progression and enhance bacterial containment upon pulmonary challenge with *Mycobacterium tuberculosis*. *J Immunol. 2007*. **178**: 7222-34.

GLUCONO-DELTA-LACTONE (GDL) INHIBITS TISSUE FACTOR AND THROMBIN DURING HUMAN BLOOD COAGULATION

GERALD NGO, CHARLES SPILLERT, PHD, SURGERY
DEPARTMENT OF SURGERY

OBJECTIVE:

Many disorders, such as sepsis or trauma, may lead to an upregulation of the coagulation cascade. The resulting procoagulant state may lead to the formation of microvascular thrombi that can disturb organ microcirculation and promote the development of organ dysfunction (2). Tissue factor is the initiator of the extrinsic coagulation pathway and is a key regulator of disseminated intravascular coagulation (2). The formation of thrombin is one of the last steps of both the extrinsic and intrinsic coagulation pathways. Thrombin itself can exert positive feedback on its own pathway by activating factors V, VIII, and XI (2), increase vascular permeability which leads to tissue damage, and inhibit fibrinolysis via activating thrombin-activatable fibrinolysis inhibitor (TAFI) (4). As a result, an up-regulation of either tissue factor or thrombin can create a procoagulant state in the patient and lead to organ dysfunction.

Currently, activated protein C is the only natural anticoagulant that has demonstrated direct activity in blocking thrombin formation, enhancing fibrinolysis, and diminishing the expression of inflammatory molecules. Glucono-delta-lactone (GDL) is a non-toxic substance that is found naturally in the human body, in many food and cosmetic products, and is on the FDA's Generally Recognized As Safe (GRAS) list. Previous studies have shown that GDL has an anticoagulant effect in blood (3). This research experiment focuses on testing GDL during procoagulant states of citrated whole blood, specifically during an upregulation of tissue factor and thrombin.

METHODS:

Human citrated whole bloods (CWB) were obtained from University Hospital's clinical labs according to IRB protocol. The bloods were pooled into samples (n=10) of approximately 1.3 mL each. Samples were gently mixed and incubated for 15 minutes at 37°C. Each sample was then divided into four aliquots of 300 uL. Each aliquot was added to cuvettes containing 32 uL of 0.1M $CaCl_2$ (to initiate clotting) and the blood concentrations listed below:

Experiment 1 (n=10)

1. 0.85% saline (Control)
2. 0.09 U/cc thrombin
3. 0.5 mg/mL GDL
4. 0.09 U/cc thrombin + 0.5 mg/mL GDL

Experiment 2 (n=10)

1. 0.85% saline (Control)
2. 0.09 U/cc thrombin
3. 1 mg/mL GDL
4. 0.09 U/cc thrombin + 1 mg/mL GDL

Experiment 3 (n=10)

1. 0.85% saline (Control)
2. 0.09 U/cc thrombin
3. 2 mg/mL GDL
4. 0.09 U/cc thrombin + 2 mg/mL GDL

Experiment 4 (n=10)

1. 0.85% saline (Control)
2. 0.045% tissue factor
3. 0.5 mg/mL GDL
4. 0.045% tissue factor + 0.5 mg/mL GDL

Experiment 5 (n=10)

1. 0.85% saline (Control)
2. 0.045% tissue factor
3. 1 mg/mL GDL
4. 0.045% tissue factor + 1 mg/mL GDL

Experiment 6 (n=10)

1. 0.85% saline (Control)
2. 0.045% tissue factor
3. 2 mg/mL GDL
4. 0.045% tissue factor + 2 mg/mL GDL

Experiment 7 (n=10)

1. 0.85% saline (Control)
2. 0.045% tissue factor
3. 0.09 U/cc thrombin
4. 0.045% tissue factor + 0.09 U/cc thrombin

Experiment 8 (n=10)

1. 0.85% saline (Control)
2. 0.045% tissue factor + 0.09 U/cc thrombin
3. 0.5 mg/mL GDL
4. 0.045% tissue factor + 0.09 U/cc thrombin + 0.5 mg/mL GDL

Experiment 9 (n=10)

1. 0.85% saline (Control)
2. 0.045% tissue factor + 0.09 U/cc thrombin
3. 1 mg/mL GDL
4. 0.045% tissue factor + 0.09 U/cc thrombin + 1 mg/mL GDL

Experiment 10 (n=10)

1. 0.85% saline (Control)
2. 0.045% tissue factor + 0.09 U/cc thrombin
3. 2 mg/mL GDL
4. 0.045% tissue factor + 0.09 U/cc thrombin + 2 mg/mL GDL

Experiments 8, 9, and 10 were repeated using plasma.

The samples were analyzed using the Sonoclot Coagulation Analyzer (Sienco, Wheat Ridge, CO, USA), a mini-viscometer that is sensitive to fibrin polymer formation and fibrinolysis (5). This instrument is currently FDA approved for evaluating human blood coagulation. Samples were evaluated for clotting time.

Clotting times were compared using GraphPad's InStat statistical program to perform paired t-tests and repeated measure analysis of variance (ANOVA). Significance was defined as test values with $p<0.05$.

RESULTS:

Experiments 1, 2, 3 – GDL's effect on thrombin during blood coagulation

Thrombin administered at doses of 0.09 U/cc final concentration significantly shortened the clotting times of all test groups ($p<0.001$). Two-tailed paired t-tests indicated a significant increase in clotting time between samples treated with thrombin versus thrombin with 0.5 mg/mL GDL ($p<0.0001$), 1 mg/mL GDL ($p<0.0001$), and 2 mg/mL GDL ($p<0.0001$) (Figure A).

Figure A: Clotting times of 0.09 U/cc thrombin and 2 mg/mL GDL treated whole bloods

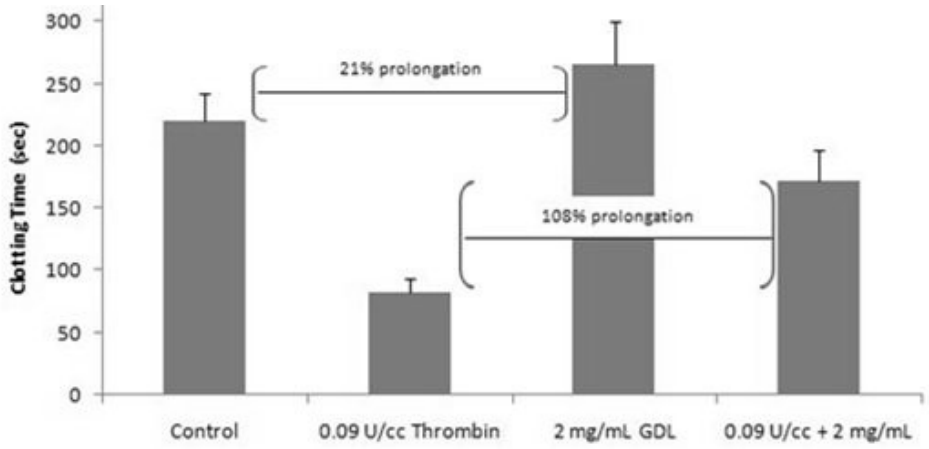

Experiments 4, 5, 6 – GDL's effect on tissue factor during blood coagulation

Tissue factor administered at doses of 0.045% final concentration significantly shortened the clotting times of all test groups ($p<0.001$). Two-tailed paired t-tests indicated a signif cant

increase in clotting time between samples treated with tissue factor versus tissue factor with 0.5 mg/mL GDL ($p<0.0001$), 1 mg/mL GDL ($p<0.0001$) (Figure E), and 2 mg/mL GDL ($p=0.0002$) (Figure B).

Figure B: Clotting times of 0.045% tissue factor and 2 mg/mL GDL treated whole bloods

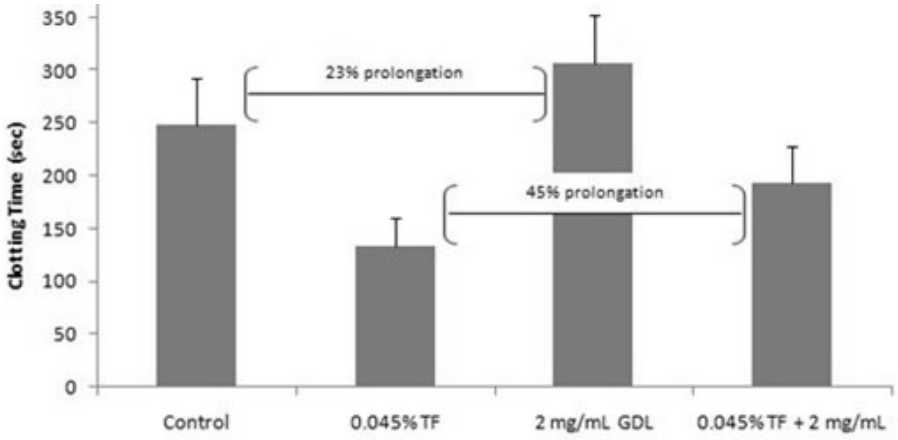

Experiment 7 – Synergistic effect of tissue factor with thrombin

Tissue factor and thrombin can contribute to decreasing clotting time without one masking the effects of the other. Two-tailed paired t-tests indicated a significant decrease in clotting time between samples treated with tissue factor versus tissue factor and thrombin ($p<0.0001$) and samples treated with thrombin versus tissue factor and thrombin ($p=0.0011$) (Figure G).

Experiments 8, 9, 10 – GDL's effect on tissue factor with thrombin during blood coagulation

Tissue factor administered at doses of 0.045% final concentration mixed with thrombin administered at doses of 0.09 U/cc final concentration significantly shortened the clotting times of all test groups ($p<0.001$). Two-tailed paired t-tests indicated a significant increase in clotting time between samples treated with tissue factor and thrombin versus tissue factor, thrombin and 0.5 mg/mL GDL ($p<0.0001$), 1 mg/mL GDL ($p<0.0001$), and 2 mg/mL GDL ($p<0.0001$) (Figure C).

Figure C: Clotting times of 0.045% tissue factor, 0.09 U/cc thrombin, and 2 mg/mL GD treated whole bloods

Experiments 8, 9, 10 in plasma – GDL's effect on tissue factor with thrombin in plasma
The procoagulant effect of tissue factor with thrombin was reduced in plasma samples treated with 0.5 mg/mL GDL ($p<0.0001$), 1 mg/mL GDL ($p<0.0001$), and 2 mg/mL GDL ($p<0.0001$).

GDL only significantly prolonged the clotting time of plasma control samples when administered at doses of 2 mg/mL final concentration (Table 1).

Table 1: GDL's effects on control

Mean Comparison	Difference	q		P value
0 GDL/0 TF/0 Thr vs 0.5 GDL/0 TF/0 Thr	-16.700	1.533	ns	P>0.05
0 GDL/0 TF/0 Thr vs 1 GDL/0 TF/0	-15.400	3.456	ns	P>0.05
0 GDL/0 TF/0 Thr vs 2 GDL/0 TF/0 Thr	-37.100	4.350	*	P<0.05

DISCUSSION:

GDL is effective during procoagulant states that involve an upregulation of tissue factor or thrombin. In practice, anticoagulants may not always be administered to patients at the commencement of the coagulation cascade but instead may be administered when coagulation is already in progress. This research experiment showed that GDL administration may prove to be useful in prolonging clotting times during these instances, especially late in the coagulation cascade when prothrombin is converted to thrombin. Additionally, GDL can antagonize different parts of the coagulation cascade simultaneously. The plasma results suggest that GDL possibly binds to tissue factor and thrombin, effectively inhibiting either from reaching its respective receptor. It is also possible that GDL functions by antagonizing a receptor site of thrombin more effectively than a receptor site of tissue factor since the addition of GDL to blood samples treated with both thrombin and tissue factor showed a prolongation increase similar to that found when GDL was added to blood samples treated with thrombin alone. However, it is not known at this time exactly what method GDL uses to oppose the effects of either thrombin or tissue factor. Future studies should further investigate the efficacy of GDL and the mechanism of GDL's anticoagulant effects.

Literature Cited

1. Amaral A, Opal S, Vincent JL. 2004. Coagulation in Sepsis. Intensive Care Medicine. Springer-Verlag; 30: 1032-1040.

2. Gando S, Nanzaki S, Sasaki S, Kemmotsu O. 1998. Significant Correlations between Tissue Factor and Thrombin Markers in Trauma and Septic Patients with Disseminated Intravascular Coagulation. Thrombosis and Haemostasis. Schattauer Verlag, Stuttgart; 79: 1111-1115.

3. Patel SG and Spillert CR. August 2007. Effects of Glucono-Delta-Lactone (GDL) on Human Blood Coagulation. Summer Research Abstracts; 138-141.

4. Siller-Matula JM, Schwameis M, Blann A, Mannhalter C, Jilma B. 2011. Thrombin as a multi-functional enzyme. Thrombosis and Haemostasis. Schattauer Verlag, Stuttgart; 106: 1020-1022, 1030.

5. Spiess BD, Spence RK, Shander A. 2006. Perioperative Coagulation Monitoring. Perioperative Transfusion Medicine. 2nd ed. Lippincott Williams & Wilkins; 349-356.

RESTING STATE FMRI AS A NOVEL BIOMARKER FOR MULTIPLE SCLEROSIS PATIENT SYMPTOMS

POOJA N. PANDIT, NILIMA SHET, NAKUL SHETH, SUSAN C. FELDMAN, PH.D.
DEPARTMENT OF RADIOLOGY

OBJECTIVE:

In multiple sclerosis (MS), abnormalities of myelin in the brain result in the formation of plaques. These plaques can be visualized using fluid attenuated inversion recovery (FLAIR) imaging. However, Blood Oxygen Level-Dependent Functional MR imaging (BOLD fMRI) may also be of use when attempting to characterize these plaques. BOLD fMRI is dependent on the functional cerebral-hemodynamic changes in the brain tissue. This poses the question, "Do the BOLD fMRI signals that correlate with plaques match the patient's active symptoms?" and "Can correlations from BOLD fMRI signals be used to identify areas where plaque may appear?"

METHODS:

Three patients were scanned with resting state BOLD fMRI while lying still for five minutes (IRB protocol #0120050110). Analysis of BOLD fMRI signals was conducted using Analysis of Functional NeuroImages (AFNI) freeware. Using AFNI the functional and anatomical scans were coregistered and the BOLD images were motion corrected and spatially smoothed. A voxel of interest (VOI) was identified within plaque and its signal characteristics were determined. Thus, locations elsewhere in the brain with highly correlated signals were identified and the distribution was correlated with clinical signs and symptoms. In addition, charts were obtained and reviewed for neurological symptoms.

SUMMARY:

Correlation Patient 1, Slice 192: Areas with a 0.61090 correlation in red

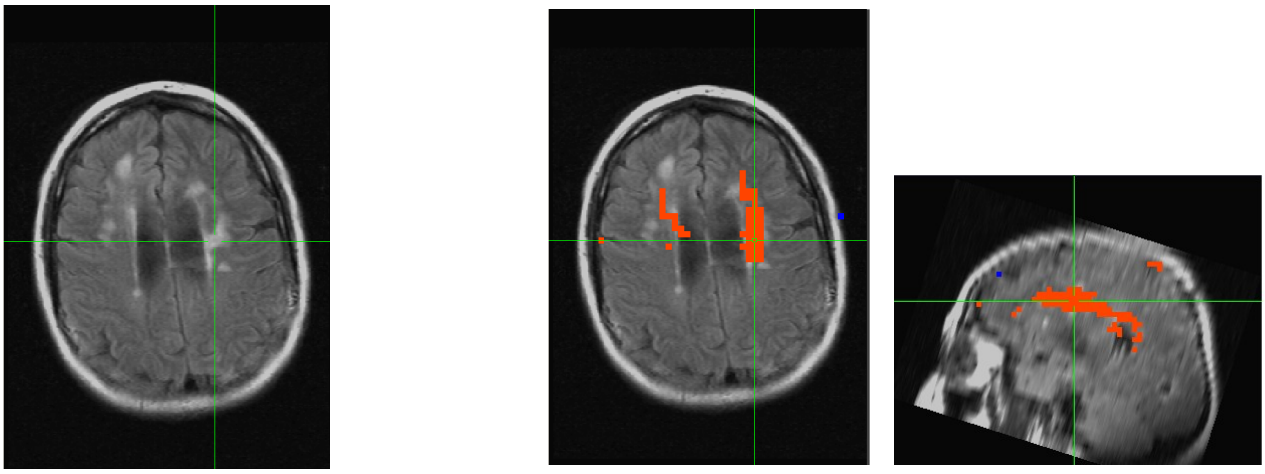

Axial 1.5 Tesla FLAIR images of the brains of MS patients were matched with their corresponding resting BOLD signal overlays. In this MS patient designated "patient 1", a VOI was selected in an MRI-identified plaque designated "plaque 1". Signals correlating to "plaque 1" with a correlation of 0.61090 were located throughout the brain in areas of MRI-identified plaque located along the ventricles and cingulated gyrus. The cingulated gyrus, part of the limbic system, is thought to play a role in emotion formation and processing, learning and memory. The patient presented with "foggy brain, increased emotional sensitivity, overall depression and little motivation".

Patient 2, Slice 109: Areas with a 0.6109 correlation in red

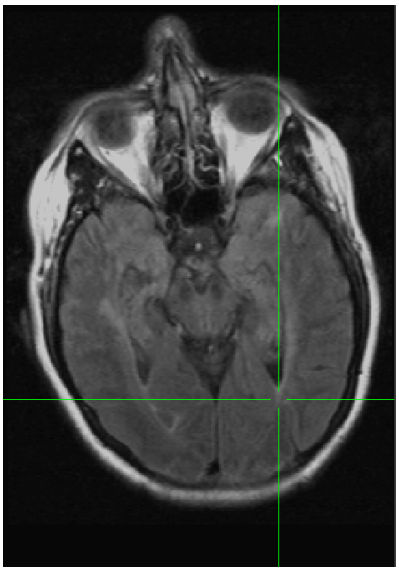

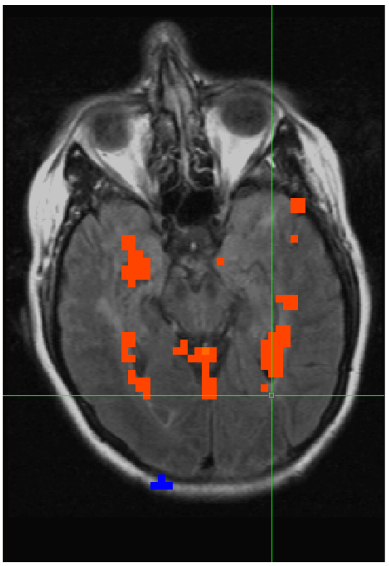

This image shows plaque located in the left occipital region (left image) which correlates to plaque located in the bilateral optic radiations with a value of 0.6109. Lin the optic radiations may produce blurred vision or dry eyes among other eye deficits. This patient, patient 2, presented with "blurred vision and dry eyes".

Correlation of BOLD fMRI signal without FLAIR-identified plaque matches patient symptoms

Patient 3: (A) VOI "A" corresponds to a confirmed periventricular and subcortical whitte matter hyperintense lesion on FLAIR and T2 sequences. (B) The BOLD signal from VOI "A" correlated to the highlighted voxels at a very high correlation (0.9485). (C) The BOLD signal calculated from VOI "A" correlated (0.9485) to the highlighted voxels (green) in the cerebellum. (D) The area of the cerebellum that correlated to the BOLD signal from VOI "A" did not have any confirmed plaque.

A. 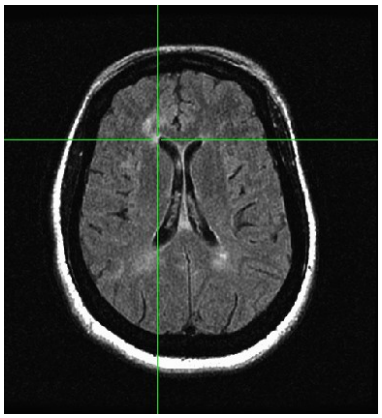

B. 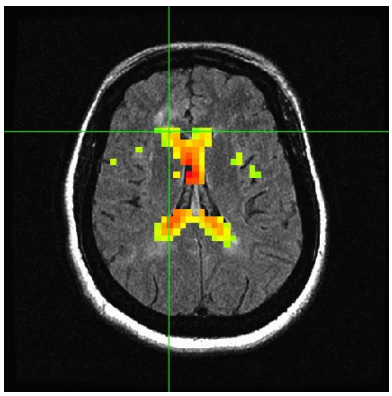

C. 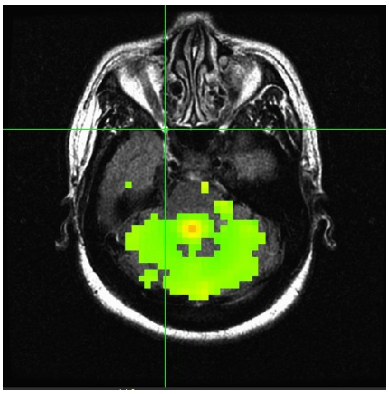

D. 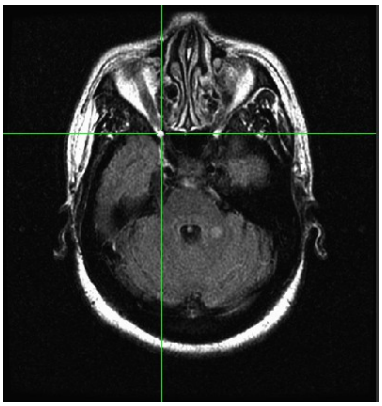

Patient 3 presented with confirmed periventricular and subcortical white matter hyperintense lesions on FLAIR and T2 sequences (shown in image A). Then, the BOLD signal from VOI "A" was correlated to the highlighted voxels at a very high correlation (0.9485), which corresponded to periventricular plaque perpendicular to the lateral ventricles. Thus, the VOI in plaque in image A can be used to identify other existing plaques. However, the BOLD signal from image A also correlated to the highlighted voxels (green) in the cerebellum (image C). This area does not have any discernable plaque, as seen in image D, and yet the patient does present with marked cerebellar symptoms such as nystagmus, abnormal gait and falls while sitting or standing. This suggests that the BOLD signal may match the patient's symptoms better than the FLAIR-identified plaque burden does. In addition, the BOLD fMRIs could be used to identify areas of future plaque in FLAIR images during the next scan that may match with symptoms that appeared before the plaque was visible.

CONCLUSIONS:

In patients with a history of MS, BOLD fMRI can be shown to identify metabolic activity of MS plaques. These specific areas where lesions cause known deficits can be linked back to the patient history and symptoms. Thus, this technique may be useful in disease monitoring and treatment. We hypothesize that BOLD fMRI signal correlates of plaque in specific brain areas can also be used to explain patient symptoms and may even have a predictive value on symptoms that may develop in the future.

DOWN REGULATION OF THE IMD PATHWAY ENHANCES STRESS RESISTANCE AND LONGEVITY IN DROSOPHILA MELANOGASTER

HARDIK PARIKH, YONGKYU PARK, PHD
DEPARTMENT OF CELL BIOLOGY AND MOLECULAR MEDICINE

PARTICIPATION DESCRIPTION:

The procedures, experiment setups, and results collection and analysis that are included within this project were all performed by me (under the guidance and supervision of Dr. Park). First, I planned out the stress resistance and longevity experiments for the various mutated strains of *Drosophila melanogaster*. I planned out three different stress experiments (oxidation, heat, and starvation), and performed each experiment 3-4 times. Only one longevity experiment was performed. I was responsible for male fly collection, virgin female (for mating different crosses) collection, transferring the flies into appropriate testing vials during experiments, and then counting them at 2-hour intervals during the stress experiments. Next, I planned and performed the gene expression studies, utilizing the procedures of RNA isolation, cDNA production, and real-time PCR. Each of these were performed greater than 8 times for the various genes tested. Lastly, I planned and carried out the fat, protein, and glycogen content assays approximately 5-7 times as well for the different flies used. I organized all of the data collected in Microsoft Excel files, performed data analysis, and created the graphs and charts to easily visualize the data. I would like to greatly thank Dr. Park in his strong guidance, teaching, patience, and support during my research experience with him.

OBJECTIVE:

Increased activation of the innate immune system is a common feature of aging animals, including mammals and *Drosophila melanogaster*. With age, *D. melanogaster* progressively express higher levels of various anti-microbial peptides (AMP). Previous studies have shown that the Immune deficient (*Imd*) pathway plays a role in the induction and regulation of the antimicrobial peptides that primarily deal with Gram-negative bacterial infections. This mechanism by which this pathway affects the aging process, however, is poorly understood. The objective of this experiment is to investigate the effects of down-regulation of the Imd pathway on stress resistance and longevity in *D. melanogaster.* The hypothesis is that down-regulation of the genes involved in the Imd pathway will result in greater stress resistance and longevity than the wild type (yw) fruit flies.

METHODS:

Stress Resistance and Longevity

Heat stress experiments were conducted by placing 2-day old males in 37°C. Starvation experiments were conducted by placing 2-day old males in 25°C without food. 200 μL of distilled H_2O were added daily. Oxidation experiments were conducted by placing 2-day old males under starvation for 6 hours at 25°C. Flies were then transferred to vials containing 300 μL of 5% sucrose, 20 mM paraquat solution to induce oxidation damage in cells. Fly counting for all three experiments was performed every 2 hours.

Fly longevity was measured by counting flies and transferring them to fresh food vials every 3-4 days until all of them died naturally.

Gene Expression

Gene expression was measured through RNA isolation, the production of cDNA, and Real-time PCR.

Nutrient Content

To measure fat, protein, and glycogen contents, 20 flies were weighed, homogenized, and used for each nutrient assay.

Results:

Figure 1: Down-regulation of the Imd gene increases stress resistance and longevity

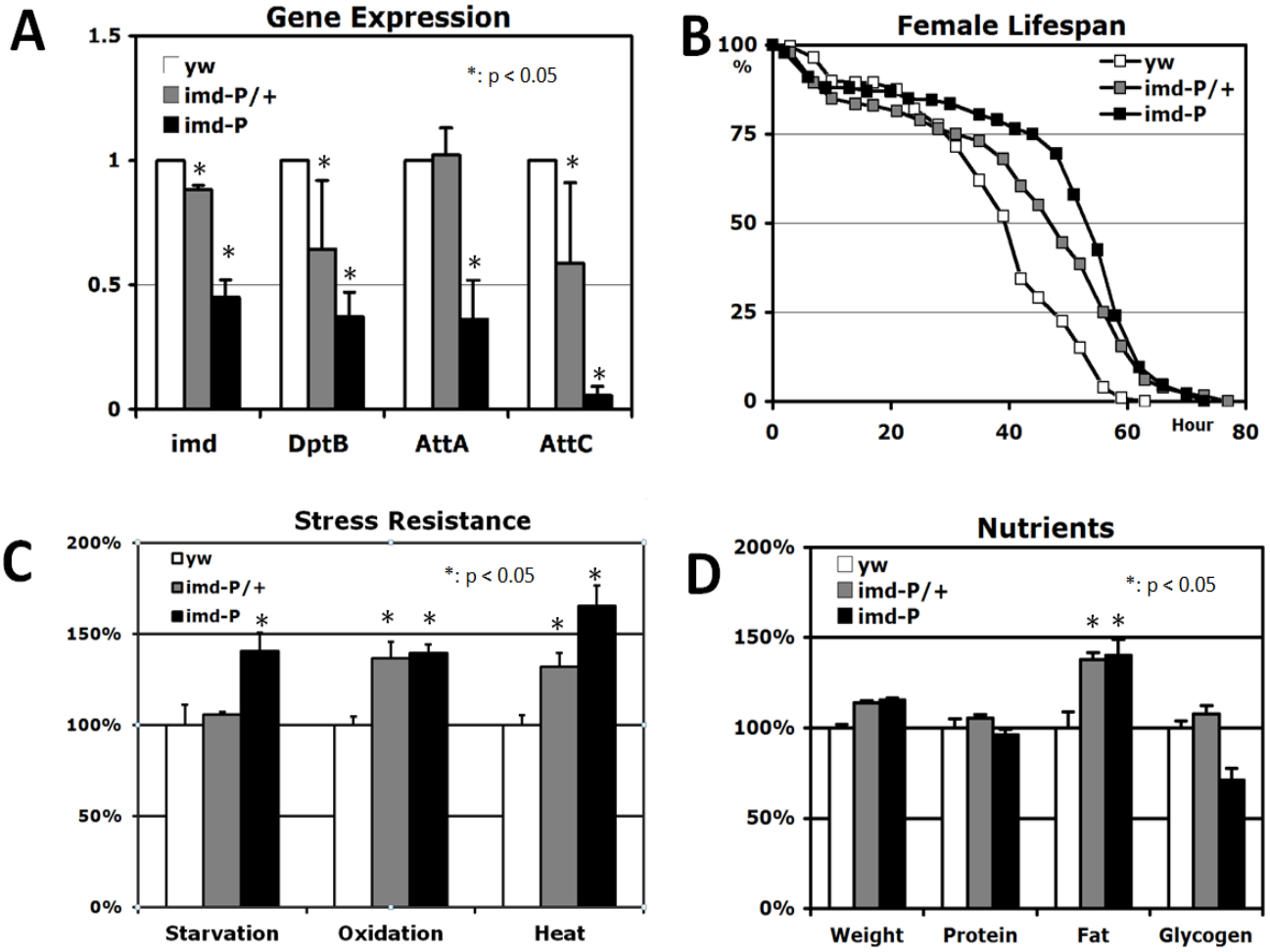

(**A**) Imd-P/+ heterozygotes generally show lower expressions of the Imd gene and its three regulated downstream genes: *DptB*, *AttA*, and *AttC*. Imd-P homozygotes show severe down-regulation of *Imd*, *DptB*, *AttA*, and *AttC*. (**B**) Down-regulation of the Imd gene enhances longevity and resistance during starvation, oxidation, and heat stress experiments (**C**). (**D**) The Imd mutants also show a significant increase in fat content as compared to the wild type flies.

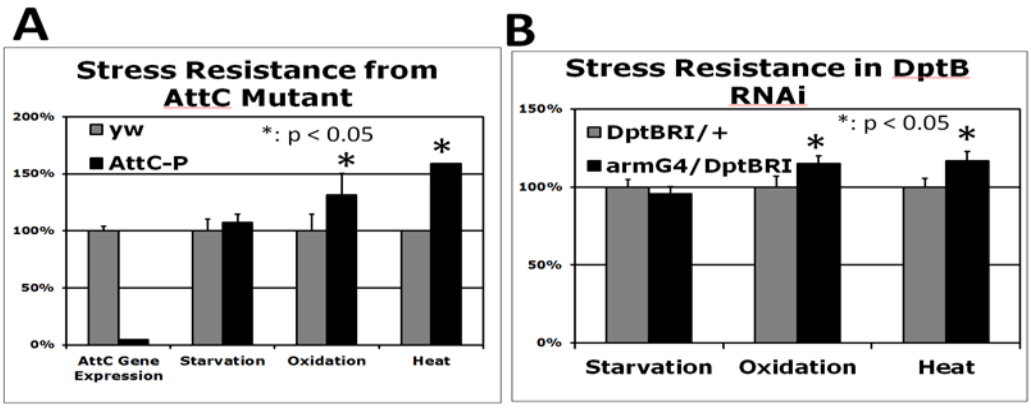

Figure 2: Decreased gene expression of *AttC* and *DptB* increases stress resistance

(**A**) The *AttC* mutant shows severe down-regulation of the *AttC* gene. These mutants have significantly increased oxidation and heat resistance, but not starvation resistance. (**B**) The *DptB* RNAi also has better survival rates in the oxidative and heat stress experiments. The *arm*-Gal4 and UAS-*DptB* RNAi were utilized in producing these flies.

Figure 3: Down-regulation of *AttC* and *DptB* gene expression have increased longevity

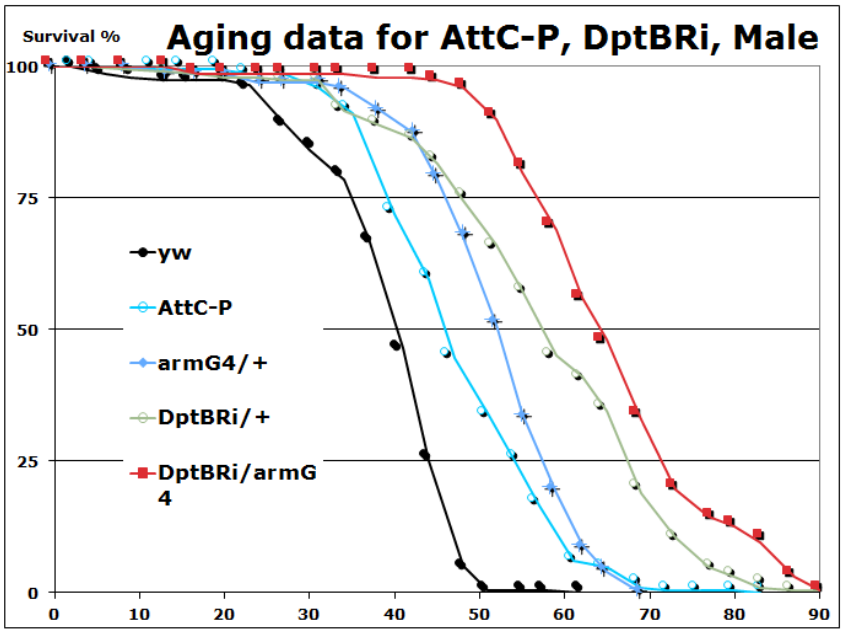

The *AttC* mutants and *DptB* RNAi demonstrate enhanced longevity compared to the control groups.

CONCLUSION:

Down-regulation of the *Imd* gene and its downstream genes (*DptB*, *AttA*, and *AttC*) enhances stress resistance and longevity in fruit flies, while also demonstrating significant increases in fat content. Previous studies have interpreted the extra fat (triglyceride) content as an adaptation mechanism for increased stress resistance and energy demands during a longer lifespan. Down-regulation of the *DptB* and *AttC* genes via *DptB* RNAi and *AttC* mutant show improved longevity and enhanced resistance to only oxidative and heat stress. This suggests that starvation resistance is more closely regulated by the upstream *Imd* gene, whereas oxidative and heat resistance are controlled via the downstream *DptB* and *AttC* genes.

REFERENCES:

Hoffmann J.A, Reichart J.M 2002 *Drosophila* innate immunity: an evolutionary perspective. Nat. Immunol. 3, 121–126.

Kim, K., Lin, Y., Park, Y, 2010. Enhancement of stress resistances and downregulation of Imd pathway by lower developmental temperature in *Drosophila melanogaster*. Experimental Gerontology 45, 984-987.

CENTRAL NEUROCYTOMA: REVIEW OF A RARE INTRAVENTRICULAR TUMOR

DHRUV M. PATEL, RICHARD F. SCHMIDT, BA, JAMES K. LIU, MD
DEPARTMENT OF NEUROLOGICAL SURGERY

OBJECTIVE:
To review available literature on central neurocytoma which are rare intraventricular tumors of neuronal origin.

METHODS:
An extensive review of literature on central neurocytoma was performed regarding their epidemiology, clinical presentation, radiological presentation, histopathological findings, molecular analysis, and options for intervention, including surgical options, radiation therapy, stereotactic radiosurgery and chemotherapy.

SUMMARY:

Central neurocytomas (CNCs) are benign tumors that represent 0.1 to 0.5% of all primary brain tumors [4,12]. More than 500 cases have been reported since they were first described by Hassoun and co-workers in 1982 [3]. They mostly affect adolescent and young adults with highest incidence in third decade [2]. Typically located in lateral ventricles of the brain near foramen of Monro, CNCs have often been misdiagnosed as oligodendroglioma and ependymoma [1,5,9]. On radiological studies, CNCs generally appears well demarcated, lobulated, and located within the lateral ventricles [12]. They typically appear as an iso to slightly hyper-dense mass on computed tomography (CT) [8] while on magnetic resonance imaging (MRI), they present as heterogeneous iso-intense to slightly hypo-intense mass on T1 and iso-intense to hyper-intense on T2 weighted images [1,8]. Glycine peak in proton magnetic resonance spectroscopy (MRS) has also been reported in CNCs, and is emerging as possible diagnostic option for these rare tumors [9]. On histological analysis, CNCs contain small to medium sized cells with indistinct cell border and small, round nuclei with granular or "salt and papper" chromatin [1]. Often honeycomb arrangement [12], irregular or neurocytic rosettes and calcification are present [11].

Definitive diagnosis of CNCs rests upon immunohistochemistry (IHC) and electron microscopy. On IHC, CNCs show positive staining for synaptophysin and neuron specific enolase while negative staining for glial fibrillary acidic protein [6]. Electron microscopy generally reveals the neuronal features of the CNCs including parallel arrays of microtubules, clear vesicles and membrane bound dense core neurosecretory granules as well as synaptic junctions [10]. Surgery is the primary treatment option and 85% local control at five years has been reported for patients with complete surgical resection. However, incomplete resection results in local control of only 46% at five years. Survival rate at five years is 99% and 86% after total resection and subtotal resection respectively. Radiation therapy significantly improves local control to 83% for tumors that are incompletely resected [7]. Stereotactic radiotherapy seems to be just as effective as conventional radiation therapy as an adjunct to surgery, however, further evaluation is needed, and chemotherapy has not been well evaluated for treatment of CNCs.

CONCLUSION:

CNCs are mostly benign tumors that affect young adults. Although radiological studies, MRS and histological analysis are used for the diagnosis of CNCs, definitive diagnosis relied upon IHC and electron microscopy to prove the neuronal characteristics of CNCs. Surgery is curative for most CNCs and complete resections brings better prognosis. Adjuvant radiation therapy can be used for tumors that are incompletely resected or for recurrences.

REFERENCES

1. Choudhari KA, Kaliaperumal C, Jain A, Sarkar C, Soo MYS, Rades D, et al: Central neurocytoma: A multi-disciplinary review. **British Journal of Neurosurgery 23:**585-595, 2009
2. Hassoun J, Soylemezoglu F, Gambarelli D, Figarella-Branger D, von Ammon K, Kleihues P: Central neurocytoma: a synopsis of clinical and histological features. **Brain Pathol. 3:**297-306., 1993
3. Kane AJ, Sughrue ME, Rutkowski MJ, Tihan T, Parsa AT: The molecular pathology of central neurocytomas. **Journal of Clinical Neuroscience 18:**1-6, 2011
4. Kim DG, Chi JG, Park SH, Chang KH, Lee SH, Jung H-W, et al: Intraventricular neurocytoma: clinicopathological analysis of seven cases. **Journal of Neurosurgery 76:**759-765, 1992
5. Lee C, Duncan VW, Young AB: Magnetic resonance features of the enigmatic oligodendroglioma. **Invest Radiol. 33:**222-231., 1998
6. Maiuri F, Spaziante R, De Caro ML, Cappabianca P, Giamundo A, Iaconetta G: Central neurocytoma: clinico-pathological study of 5 cases and review of the literature. **Clinical Neurology and Neurosurgery 97:**219-228, 1995
7. Rades D, Fehlauer F: Treatment options for central neurocytoma. **Neurology. 59:**1268-1270., 2002
8. Schmidt MH, Gottfried ON, von Koch CS, Chang SM, McDermott MW: Central Neurocytoma: A Review. **Journal of Neuro-Oncology 66:**377-384, 2004
9. Shah T, Jayasundar R, Singh VP, Sarkar C: MRS characterization of central neurocytomas using glycine. **NMR in Biomedicine 24:**1408-1413, 2011
10. Shimura T, Mori O, Kitamura T, Kobayashi S, Sanno N, Teramoto A, et al: Central neurocytoma expressing characteristics of ependymal differentiation: electron microscopic findings of two cases. **Medical Electron Microscopy 36:**98-105, 2003
11. Vasiljevic A, Francois P, Loundou A, Fevre-Montange M, Jouvet A, Roche PH, et al: Prognostic factors in central neurocytomas: a multicenter study of 71 cases. **Am J Surg Pathol. 36:**220-227., 2012
12. Ya**Ş**argil MG, Ammon Kv, Deimling Av, Valavanis A, Wichmann W, Wiestler OD: Central neurocytoma: histopathological variants and therapeutic approaches. **Journal of Neurosurgery 76:**32-37, 1992

MULTIMODAL THERAPY FOR CEREBRAL ARTERIOVENOUS MALFORMATIONS IN PREGNANCY

MANAN SHAH, NITIN AGARWAL, B.S. [1]***, GRANT SHALET, B.A.*** [4]***,***
CHARLES J. PRESTIGIACOMO, M.D., F.A.C.S. [1,2,3]***, CHIRAG D. GANDHI, M.D.*** [1,2]
[1]***DEPARTMENT OF NEUROLOGICAL SURGERY***
[2]***DEPARTMENT OF RADIOLOGY***
[3]***DEPARTMENT OF NEUROLOGY AND NEUROSCIENCE***
[4]***DEPARTMENT OF BIOLOGY, WASHINGTON UNIVERSITY , ST. LOUIS, ST. LOUIS, MO***

PARTICIPATION DESCRIPTION:

My role in this project was to create a clinical case report for a unique neurosurgical presentation, which in this case was a cerebral arteriovenous malformation during pregnancy. I had to review two past cases that the neurosurgery department was presented with and understand what treatments were done and why. This required extensive research on the history, epidemiology, etiology, and treatment options for cerebral arteriovenous malformations. It also required reviewing journal articles about the increased risk that arteriovenous malformations caused during pregnancy. Overall, the goal was to present a case report that discussed the best type of therapy for cerebral arteriovenous malformations in pregnancy.

INTRODUCTION:

An arteriovenous malformation (AVM) is a rare, congenital anomaly most commonly found in the brain, consisting of an abnormal connection between arteries and veins. This dangerous vascular lesion is prevalent in approximately .01% of the general population, affecting both men and women at about the same rate.[1-3] It has been stated that the development of an AVM might be the effect of one or several triggers on a gene defect of the post-capillary endothelium.[2] AVMs typically develop in the third week of fetal development and are frequently asymptomatic.[4] AVMs account for 1-2% of all strokes,[1] and about 53% present with a hemorrhage during their lifetime.[1, 3] Other clinical presentations include seizures and neurological deficit.[3] The modifications in maternal cardiovascular physiology that occur during pregnancy may impose a threat to the stability of the cerebral AVM and increase the risk of hemorrhage. It has been proposed that the increased cardiac output or circulatory effects of the elevated estrogen levels may be the link between AVM rupture and pregnancy.[5] The authors present two cases that portray the management dilemma that is encountered from cerebral AVMs during pregnancy. Specific therapeutic strategies are also addressed with consideration of vascular changes during pregnancy.

SUMMARY OF CASE:

CASE 1

A 27 year old G1P0 woman at 11.5 weeks gestation presented to the ER with post-coital sudden onset headache accompanied by numbness/tingling in left upper extremity. Her exam upon presentation was significant only for decreased sensation in her left upper extremity. Despite being gravid, head CT was indicated due to her clinical status, which showed right-sided periventricular intraparenchymal hemorrhage (IPH) with bilateral IVH (Figure 1a). CT angiography of the head showed Spetzler-Martin Grade IV AVM located at the right lentiform nucleus and right thalamus (Figure 1b). Her initial treatment included an external ventriculostomy drain (EVD). Follow-up head CT in the following month showed a reduction of the hemorrhage, thus not warranting an immediate ventriculoperitoneal shunt (VPS). Following an uncomplicated Cesarean delivery, the patient's neurologic status was intact except for minor memory deficits. She decided to postpone any intervention regarding her IPH.

CASE 2

A 26 year old G4P2012 woman with a history of stage 2 embolization of a left parietal AVM developed worsening of symptoms including severe migraines with concomitant vomiting, dizziness, and right-sided weakness during her pregnancy. CT angiography of the head showed a large AVM located in the left posterior parietal cortex without evidence of intracranial hemorrhage (Figure 2). She underwent an uncomplicated Cesarean delivery at 36 weeks and resumed stage 3 embolization 9 months after her delivery. Significant improvement in her concentration was noted; however, embolization had to be postponed due to another pregnancy. During this pregnancy, she suffered left arm rigidity with occasional twitches. It was later ascertained that she was non-compliant with her phenytoin seizure prophylaxis. After delivery, she reported right visual field deficits in both eyes. She continued her embolization regimen, completing stage 6 ten months ago, and recently underwent stereotactic radiosurgery. She continues to suffer migraine headaches and is closely being followed.

DISCUSSION

Cerebral AVMs in pregnant women may warrant an increased level of caution due to the greater risk of hemorrhage. Given the increase in cardiac output during pregnancy and labor, it is believed that the fragile AVM loses stability and becomes more susceptible to rupture.[4] While increased risk is indefinite, these two case reports demonstrate the caution with which AVMs must be treated in pregnant women. More specifically, multidisciplinary therapy catered to the patient would likely be useful in pregnant women with AVMs due to the dynamic nature of the lesions.[1]

In Case 1, the patient presented with the hallmark symptom of cerebral hemorrhage, a sudden and severe headache.[1] Thus, a CT angiography was done, and an initial treatment of EVD was determined to be suitable. In this case, surgical intervention was risky, given the patient's grade of IV on the Spetzler-Martin scale.[1] This scale is utilized to grade AVMs on the basis of three traits predictive of surgical outcomes: the maximum diameter of the AVM, its location (within or outside the eloquent core), and the presence or absence of deep venous drainage.[1] Some series have reported that the hemorrhage rate from AVMs in pregnancy is around 0.6% to 3.5%, which is similar to the 2% to 4% rate in non-pregnant women.[5] Therefore, since this is considered a low risk of hemorrhage, most authors suggest a conservative management of unruptured AVMs in pregnancy.[5] A more demanding method, however, is required when a pregnant woman presents with a ruptured AVM because the risk of re-bleed during the same pregnancy (27% to 30%) is much greater than the risk of re-bleed in non-pregnant women within one year of their initial bleed (6%).[5] In this woman's case, the hemorrhage had already occurred, increasing the risk of re-bleeding and the need to eradicate the AVM. Ultimately, an EVD was done for the patient, and she suffered no complications and the overall outcome of the procedure was successful reduction of the hemorrhage.[1, 3]

In Case 2, CT angiography revealed the presence of a large AVM located in the left posterior parietal cortex. However, the patient had not yet suffered a hemorrhage. Thus, an invasive procedure was deemed to be unnecessary and endovascular embolization was instead implemented; most authors suggest a conservative management of unruptured AVMs in pregnancy.[5]

However, it is not clear whether the AVM was cured in the patient. Following this initial treatment, the patient postponed her emoblization and eventually revealed that she had not been compliant with her phenytoin seizure prophylaxis. She suffered upper extremity rigidity and twitching, visual field deficits and recurrence of migraines. It is uncertain whether there exists a correlation between the patient's inconsistent therapy and her neurological decline.

However, the positive outcome of her initial treatment cannot be ignored. Pregnant women with AVM, who have not yet suffered a hemorrhage, would benefit with endovascular embolization.

CONCLUSION:

Improvements in the neurosurgical field provide great options for treating AVMs, including microsurgery, radiosurgery, and embolization. The most effective method in the management of AVMs during pregnancy is a multifaceted approach, which is tailored to the individual patient. A close collaboration with a group of obstetricians, neuroradiologists, anaesthesiologists, and neurosurgeons is necessary to be successful.

REFERENCES:

1. Friedlander RM. Arteriovenous malformations of the brain. *New England Journal of Medicine*. 2007;356:2704-2712
2. Söderman M, Andersson T, Karlsson B, Wallace MC, Edner G. Management of patients with brain arteriovenous malformations. *European journal of radiology*. 2003;46:195-205
3. Fleetwood IG, Steinberg GK. Arteriovenous malformations. *The Lancet*. 2002;359:863-873
4. English LA, Mulvey DC. Ruptured arteriovenous malformation and subarachnoid hemorrhage during emergent cesarean delivery: A case report. *AANA J*. 2004;72:423-426
5. Trivedi RA, Kirkpatrick PJ. Arteriovenous malformations of the cerebral circulation that rupture in pregnancy. *Journal of Obstetrics & Gynaecology*. 2003;23:484

Figure 1a. Non-contrast head CT, axial cut, of 27 year old G1P0 woman. Note right thalamic intraparenchymal hemorrhage with intraventricular hemorrhage.

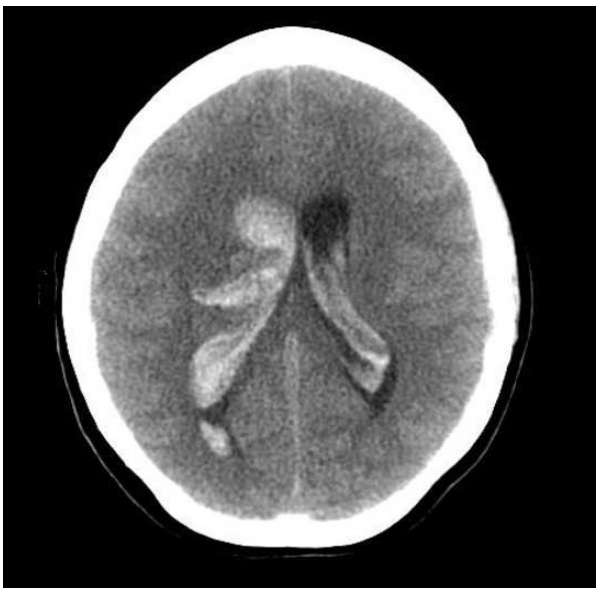

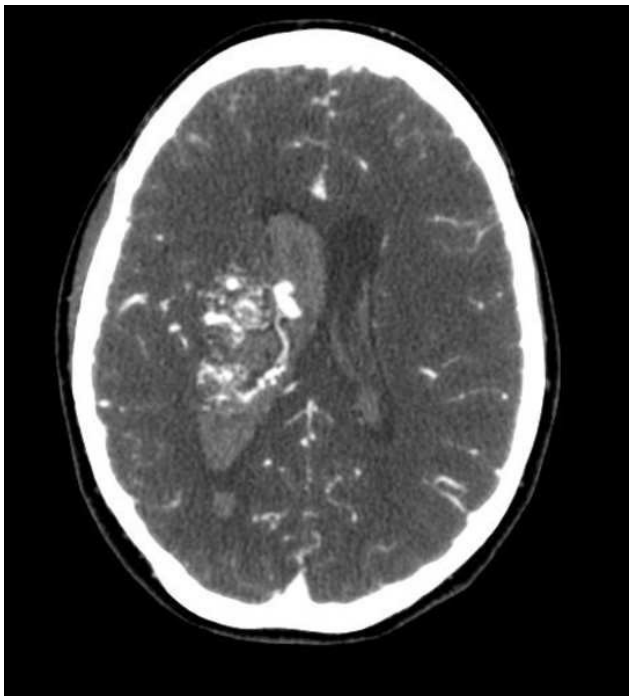

Figure 1b. CT angiography of the head, axial cut, of 27 year old G1P0 woman. Note presence of AVM in right lentiform nucleus and right thalamus.

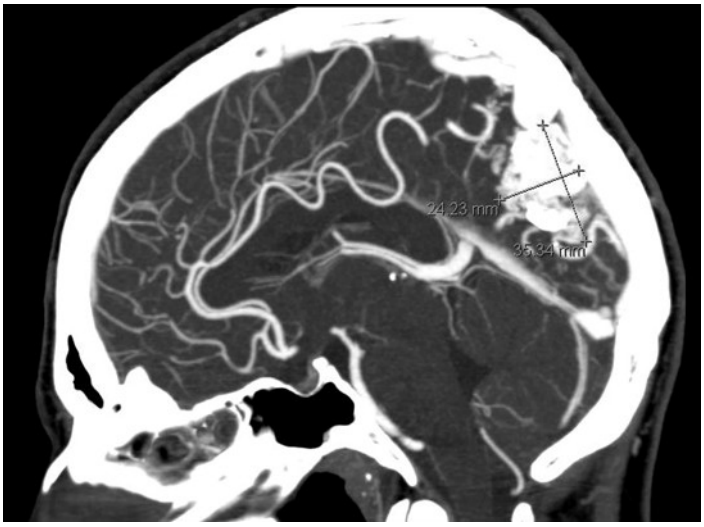

Figure 2. CT angiography of the head, sagittal cut, of 26 year old G4P2012 woman. Note presence of left posterior parietal AVM with prior stage 2 embolization.

A META-ANALYSIS OF DRUG ELUTING STENTS VS. BARE METAL STENTS FOR TREATMENT OF EXTRACRANIAL VERTEBRAL ARTERY DISEASE

NAKUL SHETH, BA, VIKAS GUPTA, MD, SHARIYAH GORDON, WENZHUAN HE, MD, CHARLES J. PRESTIGIACOMO, MD AND CHIRAG D. GANDHI, MD
DEPARTMENT OF NEUROLOGICAL SURGERY

BACKGROUND

Although a growing number of reports offer evidence for the potential of drug eluting stents (DES) in treating atherosclerotic stenosis of the extracranial vertebral artery, their efficacy when compared to bare metal stents (BMS) is uncertain due to the lack of a large prospective randomized trial.

METHODS

A search strategy was used using the terms "stents," "drug-eluting stents," "atherosclerosis," "vertebral artery," and "vertebrobasilar insufficiency" through Medline. Five studies met the criteria for a comparative meta-analysis. The technical and clinical success, periprocedural complications, target vessel revascularization (TVR), rates of restenosis and recurrent symptoms and overall survival were compared between the DES and BMS groups using the Mantel-Haenszel method with fixed and random effect models.

RESULTS

The mean pretreatment stenosis was 83.8±4.2% in the DES group (n = 156) and 80.12±2.7% in the BMS group (n = 148). There was no significant difference in the technical success (OR = 1.528, p = 0.622), clinical success (OR = 1.917, p = 0.274) and periprocedural complications (OR = 0.741, p = 0.614) between the two groups. The rates of technical success, clinical success and periprocedural complications were 98.78%, 95.77% and 1.94% for the DES group vs. 100%, 97.96% and 2.96% for the BMS group. There was no periprocedural mortality, stroke or TIA. The mean clinical and radiological follow-up times were 19.1±6.9 and 14.23±1.5 months respectively, for the DES arm and 26±7.6 and 20.5±3.3 months, respectively, for the BMS group. A 0.388 odds ratio of no-restenosis in the BMS to DES arms (p = 0.001) indicated a significantly higher restenosis rate in the BMS group relative to the DES group (33.57% vs. 15.49%, respectively). When compared with the DES group, the BMS group had a significantly higher rate of recurrent symptoms (2.76% vs. 11.26%; OR = 3.319, p = 0.011) and TVR (4.83% vs. 19.21%; OR = 4.099, p = 0.001). There was no significant difference between overall survival (OR = 0.655, p = 0.32).

CONCLUSION

A lower rate of restenosis, recurrent symptoms and target vessel revascularization was noted in the DES group.

EFFECTS OF ANTI-INFLAMMATORY DRUGS ON BONE REGENERATION

BAILEY SU, CHRISTELLE TAN, JESSICA COTTRELL, J. PATRICK O'CONNOR
DEPARTMENT OF BIOCHEMISTRY AND MOLECULAR BIOLOGY

INTRODUCTION

There are over 6 million bone fractures in the United States each year, many of which develop complications in the form of delayed healing or failed healing. Identifying new drugs or drug targets that can accelerate or enhance the bone regeneration process would have a significant impact on patient care and quality of life.

The arachadonic acid (AA) cascade is a well-established but complicated pathway. It involves pro- and anti-inflammatory processes, which must be balanced in order for proper bone regeneration to occur. Two groups of end products of the AA pathway are prostaglandins and leukotrienes. The formation of prostaglandins has been shown to aid fracture healing, while the formation of leukotrienes has been shown to inhibit it. Inhibition of the leukotriene pathway can enhance fracture healing, making it a strong candidate for clinical drug development.

In our experiment, we look to explore how the use of anti-inflammatory drugs to inhibit leukotriene formation affects bone regeneration. ABT-761 and DG-051B both inhibit leukotriene production at different points along the pathway; the former acting on 5-lipoxygenase (5-LO) and the latter acting on leukotriene A4 hydrolase (LTA4H). We hypothesize that ABT-761 and DG-051B will both accelerate fracture healing when compared to the placebo.

BACKGROUND

It has been previously shown that inhibition of 5-LO accelerates fracture healing. LTA4H is another enzyme of the arachidonic acid pathway that works downstream of 5-LO and catalyzes the conversion of LTA4 to LTB4. Because LTA4H works downstream of 5-LO, it has become an attractive drug target due to the potential for reduced side effects.

DG-051B is a selective LTA4H inhibitor that may accelerate fracture healing. Because DG-051B selectively inhibits LTA4H, only LTB4 synthesis is reduced without affecting the synthesis of other leukotrienes or lipoxins.

METHODS

48 female Sprague-Dawley rats, weighing an average of 294 grams, were used for this experiment. A 0.7 mm diameter stainless steel rod was inserted anterograde into the femoral canal through the proximal end of the femur. (Figure 1). This method of rod insertion is in contrast to the traditional method which goes through the knee joint. There were many advantages to the new technique, including a diminished inflammatory reaction, a reduction in surgery time, and no need for sutures. All of these factors made the anterograde insertion a more favorable technique for rod implantation because it increased efficiency , decreased risk of infection, and did not affect knee or hip function.

After surgery, the rats were allowed to heal for 7 days. On the 7th day (experimental Day 0), the rats were anesthetized and their femurs fractured using a custom-made 3-point bending apparatus (Figure 2).

Beginning four hours post-surgery, the rats were treated with DG-051B, ABT-761 or placebo by oral gavage. 1% hypromellose was used as a carrier, and the drug or placebo was given as a 1 ml solution twice-a-day (morning and early evening) for 21 days. The rats receiving DG-051B were given 3 mg/kg twice a day, and the rats receiving ABT-761 were given 5 mg/kg twice a day. Serial x-ray examination of live animals occurred at 1 and 2 weeks, and will continue for weeks 3, 4 and 5 after fracture. Rats will be euthanized at 3 and 5 weeks after fracture and the femurs will be harvested for microcomputerized tomography, histomorphometry, and mechanical testing.

RESULTS

In the upcoming weeks there will be more testing to determine final results; biomechanical testing at 3 and 5 weeks will provide an objective outcome measure. For now, the two-week x-rays show considerable callous formation in the DG-051B and ABT-761 treated rats (Figure 3). While there is also callous formation in the rats given placebo, the growth does not seem as accelerated as it is in the other rats. Additionally, there is more bone growth within the fracture site of the drug-treated rats. This is demonstrated by the presence of the large gap that persists between the two ends of bone in the placebo rats, but which is not present in the drug-treated rats.

CONCLUSIONS

Figure 1.

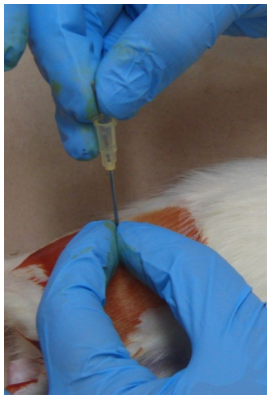

Figure 2.

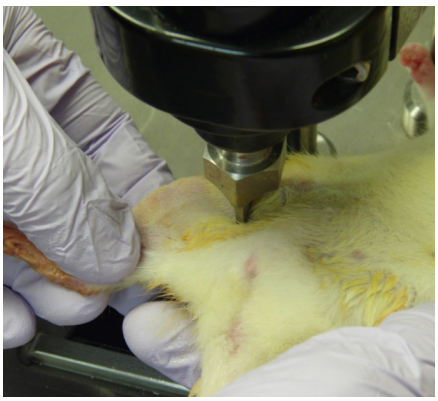

Figure 3.

DG-051B ABT-761 Placebo

In this ongoing project, some preliminary conclusions can be drawn at this point. First, ABT-761 and DG-051B are effective oral agents for accelerating bone regeneration, and have strong potential as candidate drugs for clinical development. Additionally, accelerated bone regeneration through use of 5-LO inhibitors appears to work by inhibition of LTB4 production and not of other leukotrienes.

UMDNJ-NEW JERSEY MEDICAL SCHOOL

2012 SUMMER STUDENT RESEARCH PROGRAM
RESPORT OF ACCOMPLISHMENTS
SUMMER STUDENT ABSTRACTS